# Natural frequency of laminated composite plates having cutout opening with lining along the cutout edges analysed using six node linear strain triangular elements optimised using aqua search meta-heuristic algorithm and machine learning gradient boosting method

**K. N. V. Chandrasekhar[1*], V. Bhikshma[2]**

[1]Department of Civil Engineering, Vasavi College of Engineering, Hyderabad, Telangana, 500031 India.

ORCID: 0000-0003-3930-1196

[2]Department of Civil Engineering, University College of Engineering, Osmania University, Hyderabad, Telangana, 500007, India.

ORCID: 0000-0003-1917-509X

**Abstract.** The use of laminates has become an integral unit in every field of Engineering. The laminated plates and shells are a common form of structural shapes which are widely used for various types of Civil Engineering purposes. The use of laminates over the long run sometimes wear out near the ends which are usually not protected. The life span of the laminate can be increased further by strengthening the boundary. Laminates having cutout are widely in use for various purposes of construction. The basic idea behind the paper is to strengthen the boundary of the laminate around the cutout opening. The strengthening can be done by increasing the number of layers, by increasing the thickness, by increasing the modulii of elasticity of the material and few other ways. This lining of laminate can increase the life span and can contribute to the performance of the laminate during its life. The present paper evaluates the fundamental frequencies of laminates having cutouts for both unlined and lined laminates along the cutout edges by increasing the number of layers near the cutout edges. Five different machine learning methods have been used to validate our study and determine the performance metrics. Coding is done in Google Colabs®. The five methods are namely Linear Regression (LR), Ridge Regression (RR), kNearest Neighbour (kNN), Random Forest (RF), Gradient Boosting (GB). The root mean square error and the $R^2$ value are determined to check the accuracy of the model. The best method is found to be gradient boosting with least error nearly equal to zero and an $R^2$ value of 99.9%. The results of non-dimensional natural frequency obtained using AIML are cross verified with the results obtained from finite element analysis using six node linear strain triangular elements. The results are encouraging and the error is nearly equal to zero in case of gradient boosting.

**Keywords:** Cutout, non-dimensional frequency, Linear strain triangle, Lining of laminate, Aqua search meta heuristic, Gradient boosting

## 1.0 Introduction

The use of laminated composites is inevitable in the field of Civil Engineering construction. The laminates are subjected to different types of loading such as mechanical loading, thermal loading, Hygroscopic loading, vibration loading and so on. The laminates are used with several different support conditions such as fixed (C), simply supported (S), hinged (H) and free (F) edges. The laminate has to perform in carrying the load as that of other construction material when it is used in a structure. The main focus of the present paper is to investigate the fundamental frequencies and mode shapes of laminates having cutouts with different boundary conditions. The laminate is discretised using six node linear strain triangular elements and the all the elements along the cutout edges are having different set of laminae compared to the rest of the laminate. This is to ensure the material will last longer and will not be subjected to wear and tear easily. This lining can be done in several ways such as increasing the number of layers along the the cutout edges, changing the modulii of elasticity of the material along the cutout edges. The present focus is only on increasing the number of layers and the modulus of elasticity in the elements along the cutout edges and investigate the fundamental frequencies and compare them with the fundamental frequencies of laminates without any change in the number of layers.

The increase in the number of layers for the elements along the cutout might pose a manufacturing constraint. The weaver has to increase the number of layers for the elements along the cutout edges. The manufacturer should be able to include this change during the manufacturing of laminates. The basic idea is to increase the life span of the laminate when used for a construction activity. The edge stiffening of the cutout can increase the resistance and improve its performance. This introduction will give a clear understanding of the proposed idea of lining of laminates by increasing the number of layers and modulus of elasticity for all elements along the edges of the cutout for different support conditions. The support conditions which are considered in this study are CCCC, SSSS, HHHH. Each type of structure as mentioned above is discussed in each of the following sub-sections. This section is outlined to efficiently describe information and basic concepts discussed in this study.

The recent papers on strengthening the open hole tensile strength have revealed that the structural performance can adversely get affected by failure at cutout or holes. Yu et.al., in 2022 [10] did his research work on using z-pins to prevent delamination damage. Experimental work on using z-pins has proved that the strain level at the notch can be reduced when compared with an unpinned specimen. There is cost factor involved to design and manufacture a z-pin and use it around the notch. There is also a chance where z-pins are not feasible to use such as wrapping a concrete member around an opening for increasing the strength of concrete member.

In this research work, we propose a new concept known as lining of laminates, where in the edges exposed in the cutout can be strengthened by increasing the number of layers along

the cutout edges. The idea is similar to the edge of the cloth, wherein the edge of the cloth has a strength higher than the cloth and there will be no delamination damage along the exposed openings. The cloth edges are stronger and prevents the tearing along the edges. Similar to this, we can strengthen the edge of a laminate by lining the laminates along the cutout or open hole edges. The main advantage of this idea, it can be used anywhere and there are no practical constraints. The main limitation of this idea is that the manufacturer has to supply standard sizes and standard samples for testing in the laboratory.

In the present study, we plot the curves to interpolate and determine the fundamental frequency for an optimal lining factor of material. The coding is done in ForTran® and MatLab® on an i7 processor laptop. The laptop has 4 cores and 8 logical processors with 8GB RAM, 1 TB hard drive and base speed of 2.59 GHz up to a top speed of 3.3 GHz. The characteristic curve clearly shows the convergence and which can be very useful to determine the lining factor for a desired frequency and vice versa. The lining is done along the edges of the cutout to increase the strength of laminate and which lowers frequency. The results are cross verified using AIML techniques. The input data is used to train machine learning algorithms. Five different machine learning methods have been used to validate our study and determine the performance metrics. Gradient boosting has been applied to determine the lining factors for other geometry ratios and predict the non-dimensional natural frequency of the laminate.

### 1.1 Need for the Study

The laminates are widely in use in several areas of Civil Engineering. They are replacing the conventional materials due to their high strength and low weight. The laminates are also wrapped around the concrete members for increasing the strength of the member. They are provided around the openings in the concrete to reduce the stress carried by the concrete. The study on the behavior of the laminates is very important for a Civil Engineer. There are few issues with laminates being used as wraps around the openings in concrete. The laminate has to be teared to the same dimensions as the opening in the concrete. The cut edges are usually having threads which are set loose as a result the laminate cannot be glued the concrete member thoroughly and the strength of the member is not as it is expected to have. Similarly these cutout openings have to be protected and we have to make sure that the laminate takes the load without failure at an early stage. Similarly, when a laminate having a cutout opening is used as a plate and when the load is applied on the laminate, the cutout edges are the first ones to tear and hence the entire laminate cannot be used to carry loads. In such cases, as well the cutout edges when they are strengthened, the laminate offer an increase in strength to carry loads. Hence, this present study is focussed on lining of laminates used along with reinforced concrete members or as a transverse plates to carry loads. There is a definite need to study the laminate with the cutout edges being strengthened by increase the number of layers of laminae in the area close to the edges. When the edges are protected, then the material inside will start taking the load and the laminated plate can be used to carry the loads. The main focus of this research study is to apply the idea of lining of laminates along the edges of the cutout and determine the fundamental frequencies for different types of shells and plates with different support boundary conditions. We need to compare the fundamental frequencies of laminates with and without lining of laminates.

### 1.2 Aims and Objectives of the Study

Keeping in view of the requirement of the need for the study, the following aims and objectives have been set out.

i. To find the non-dimensional natural frequency of the CCCC composite laminated shell with lining around the cutout opening

ii. To calculate a lining factor for a desired frequency of the CCCC laminated composite shell using aqua search meta-heuristic optimisation algorithm

iii. To develop interpolation curves with different geometry ratios and determine non-dimensional natural frequency of the CCCC composite laminated plate with lining material along the cutout opening

iv. To apply AIML techniques and determine the non-dimensional frequency for a chosen a/b ratio, a/h ratio and lining factor and compare with the FEM result.

### 1.3 Scope of the study

i. The study is within the scope of CCCC laminated composite plates with 0/90/0/90 lamina.

ii. The laminated composite plates are having eight layers of 0/90/0/90/0/90/0/90 for all the elements in the lining zone and along the cutout edges. The laminate is having four layers of 0/90/0/90 for the remaining portion of the plate.

iii. The non-dimensional fundamental frequency and mode shape with the maximum nodal displacement for the first mode of vibration is determined without increasing the modulii of elasticity and also by increasing the modulii of elasticity for the elements along the edge of the cutout.

iv. The study is limited to linear elastic static analysis only.

v. The Poisson ratio to remain constant and lining factor to remain constant for a given laminate.

## 2.0 Literature review

The need of laminated composites in the field of Civil Engineering cannot be under emphasised. The use of laminated composites in the field of structural engineering has rapidly increased by replacing the structural outfits with laminated composite specimens due to their light weight, high strength to weight ratio, low corrosion, longevity, and low coefficient of thermal expansion. [9] Cutout edges of FRP composite with threads loosened and the bond is weak between concrete and composite laminate as shown in Fig.1. Laminated composites testing in the laboratory to determine the frequency as shown in Fig.2.

**Fig.1 Cutout edges of FRP composite with threads loosened and the bond is weak between concrete and composite laminate [9]**

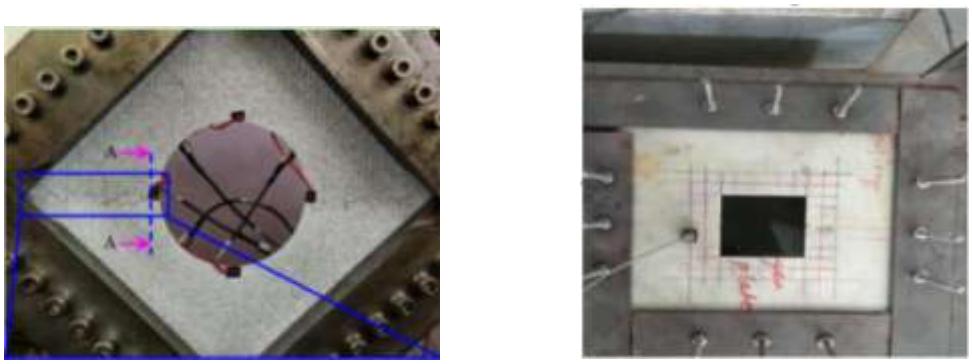

**Fig.2 Laminated composites testing in the laboratory to determine the frequency [source online]**

Cutouts are made to lighten the structure, to provide the access the different parts of the structure, changing resonant frequency, and for ventilation [6]. Sharmila sahoo [1] did research on free vibration characteristics of stiffened composite hyperbolic paraboloid shell panel with cutout and presented the mode shapes. Eight node curved beam element is used to analyse cross ply and angle ply laminates. The study on natural frequencies can be used to develop design aids for structural engineers. This study provides the specific zones within which the loss of frequency is less than 5%-10% the frequency with a central cutout. Hachemi and Hamza-Cherif (2020) [5] present their research work on free vibration characteristics of laminated composite square plates having complicated cutouts using higher order shear deformation theory coupled with a curved quadrilateral p-element. The fundamental frequencies were studied for different characteristics of plate such as cutout shape, plate thickness, fiber orientation angle, and boundary conditions. Maharudra et.al. (2020) [2] focussed on the buckling behavior of composite trapezoidal laminates panel with cutouts, subjected to nonuniform in-plane loads. The effect of various parameters such as cutout size, boundary condition, plywood orientation of panel is studied in greater detail. Ahmad et.al. (2013) [8] studied the effect of centrally located cutout and cracks emanating

from the cutout on the free flexural behavior of the plate. The circular and the elliptical cutouts, crack length, thermal gradient with different boundary conditions have been studied in detail. The properties of functionally graded material are evaluated using Mori-Tanka scheme and the plate kinematics is based on the first order shear deformation theory. Sundarajan and Pratik (2013) [3] studied the effect of moisture concentration and thermal gradient on free vibration characteristics and buckling of laminated composites. The effect of plate geometry, cutout geometry, moisture concentration, thermal gradient and boundary condition is numerically studied. Tarun kant and Swaminathan [18] in the year 2001 presented an analytical solution to find the natural frequency of the laminated composite. Sharmila sahoo [1] did her research work on free vibration characteristics of stiffened hyperbolic laminated composite plates having cutouts in different shapes. Eight noded curved shell element with a three node curved beam element is used to model the laminated composite shell panel with different shapes and sizes of cutouts. The effects of these parameters on fundamental frequencies are considered in detail. The design aids for laminated composites can be prepared for structural engineers. The practising engineers can use these results when designing a cutout opening in the laminate.

Aydin Komur et.al., [4] did their research study on buckling analysis of a woven glass polyster laminated composite plate with a hole. An elliptical/circular hole is applied and tested for various plates both in shape and position of elliptical hole. They found that the increasing of hole positioned angle caused to reduce the buckling load. Mohammed salih et.al., [7] did their study on free vibration analysis of perforated laminated composite plates. They worked on three support conditions namely SSSS,CCCC,SCSC. They effect of number of holes and hole area ratio, lamination angles and boundary conditions on vibration has been investigated in greater detail. The lamination angle has a clear effect on the change in the natural frequency of vibration.

The open hole tensile strength can be increased by using the lining of laminates to strengthen the edges, which is similar in blue color along the edge as shown in the image given here. This is quite suitable for the case of thin laminates. For example, the laminated composite wrap around the opening of a concrete beam is a thin laminate. The laminated composite. Oskana and Andrey [11] did their research work on prediction of stress strain state of a rectangular plate with a circular cutout. They used principal component analysis and convolutional neural networks. They estimated the mean square error loss function for both train data set and test data set up to 500 epochs. Input and hidden layers use hyperbolic tangent function as activation. Eight neurons are used to process float data and 76 neurons are used to process categorical data. Lakshmi narayana et.al. [12] did their study on thermal buckling analysis of composite laminated plates having square or elliptical openings. They have used a 16 ply quasi isotropic graphite epoxy symmetrically laminated composite plates. They found that for a rectangular laminated composite plate having a elliptical cutout opening, the magnitude of thermal buckling increased as the cutout orientation has increased from 0 to 90 degrees. Yassine El Kiri et.al., [13] developed an artificial neural network to predict the external corrosion, predict the burse pressures thus avoiding the need for complex finite element analysis any more and any further. The results indicated that the parabolic shape is the most crucial parameter and is generally more detrimental to the structure. Agim Seranaj et.al., [14] did present their research work to find the optimal size and position of openings in the reinforced concrete structure based on stress, displacement, and boundary

cases. Several examples on the optimisation of shells with advanced algorithms is done to validate their research work. Their research has reduced the weight of the structure by nearly 30% - 40% by providing openings in the structure. Vidhya Ramesh et.al., [15] developed a code using artificial neural networks to predict the compressive strength of a sustainable recycled concrete. Recycled aggregates concrete and treated textile waste water are used for eco-friendly concrete. Training and testing of model is done using experimental data compiled on eco-friendly concrete. The validation of the model is done by comparing the experimental results with the ANN predictions and these are found to be close.

Benbokhari Abdellatiff et.al., [16] used artificial neural networks (ANN) to predict the seismic response of structures subjected to earthquake events. Three ANN models were used which are a hybrid of both supervised and unsupervised learning. Auto encoder ANN performed better than principal component analysis with ANN, PCA-ANN and ANN models. They are able to quickly and accurately predict the seismic responses of structures for unforeseen ground motion using only the building characteristics. Arun et.al. [17] used several machine learning algorithms, specifically Random Forest (RF), Gradient Boosting (GB) and Extreme gradient boosting (EGB) to predict the compressive strength is the main focus of their study. They judged their model's performance by calculating mean average error (MAE), root mean square error (RMSE) and $R^2$ values. The developed a powerful tool to predict the compressive strength in various scenarios. Gao et.al., [10] did their research study on designing and fabricating Z-pins to improve the open hole strength of a laminated composite. The cutouts cause damage to structural performance and their study of the behavior and response of the laminated composite having cutout openings is inevitable. Gao et.al., proposed fine Z-pins arrangement around the cutout opening to increase the strength of the opening when the CFRP laminated composite is subjected to axial loading as shown in Fig.3. The open hole in the laminate will definitely reduce the strength bearing capacity and the laminate will fail at the opening. They tested using fine z-pin made of T800S fibres having about 240 individual fibres with the volume fraction of 62% and the diameter of single filament is 5 μm. ASTM D3039 standard is used to conduct the tensile test of the specimens. The use of z-pins has increased the open hole strength by 9% and 54.1% reduction in the delamination damage area.

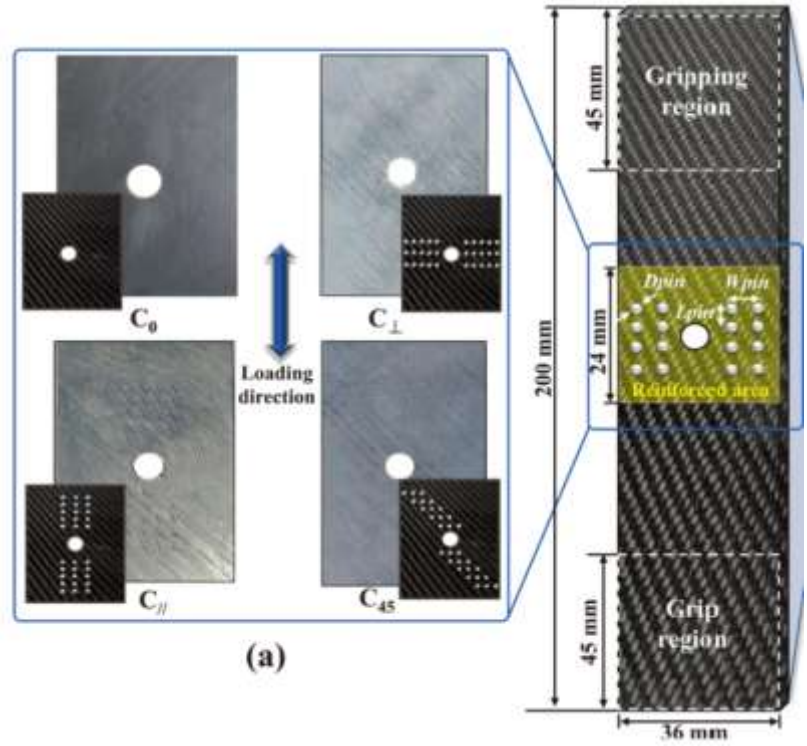


**Fig.3 Dimension of Z pinned OHT specimens prior to damage [10]**

## 3.0 Methodology

The proposed way is to increase the stiffness and density of the elements along the length of the edge of cutout in order to reduce the displacement produced due to vibration. The laminated composite plate is having a dimension of 80 x 80 square and the dimension of cutout opening is 30 x 30 square at the centre of the plate. The entire plate is meshed using first order six node linear strain triangular elements. The elements along the edge of the cutout are having eight layers of lamina 0/90/0/90/0/90/0/90 and the modulii of elasticity are multiplied by 20. The remaining portion of the laminated composite plate has four layers of lamina 0/90/0/90 as shown in the Fig.4. The dynamic analysis is performed. The stiffness matrix, mass matrix are calculated for each element and then assembled to obtain a global stiffness matrix and global mass matrix. The flowchart to perform the static analysis is as shown in the Fig.5. The coding in developed using VC++, ForTran® and Matlab® on Intel® Core™ i7-6700HQ CPU @ 2.60GHz.

https://doi.org/10.5281/zenodo.18617512

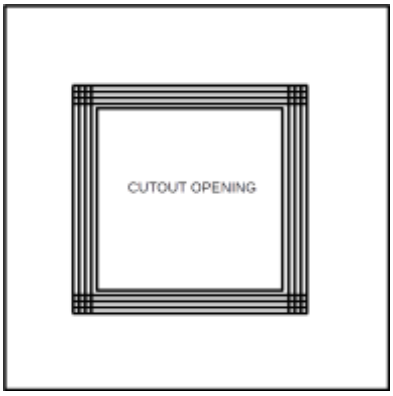


**Fig.4. Lining of laminate around the cutout edges**

Find the fundamental frequency , with usual notations $\left|\boldsymbol{K}-\boldsymbol{M}\omega^{2}\right|=\mathbf{0}$

Non-dimensional frequency = $\omega^{0.5}a^{2}\sqrt{\dfrac{\rho}{E_{YY}\,h^{2}}}$ (1)

The mode shape can be determined using eigen vector obtained by the relation

$$\boldsymbol{K}x=\omega^{2}\boldsymbol{M}x \tag{2}$$

Determine the Optimal lining factor for a desired frequency

With usual notations, $K = M\,\omega^{2}$ and $\bar{\omega} = \omega\, a^{2}\,(\rho/E_{22}h^{2})^{1/2}$

Where ‘K’ is the stiffness matrix and ‘M’ is the mass matrix

‘ω’ is the natural frequency

‘$\bar{\omega}$' is the non-dimensional frequency (NDF)

‘a’ is the length of each side

‘h’ is the thickness of the laminate

The variable is lining factor for each iteration and determine the natural frequency

https://doi.org/10.5281/zenodo.18617512

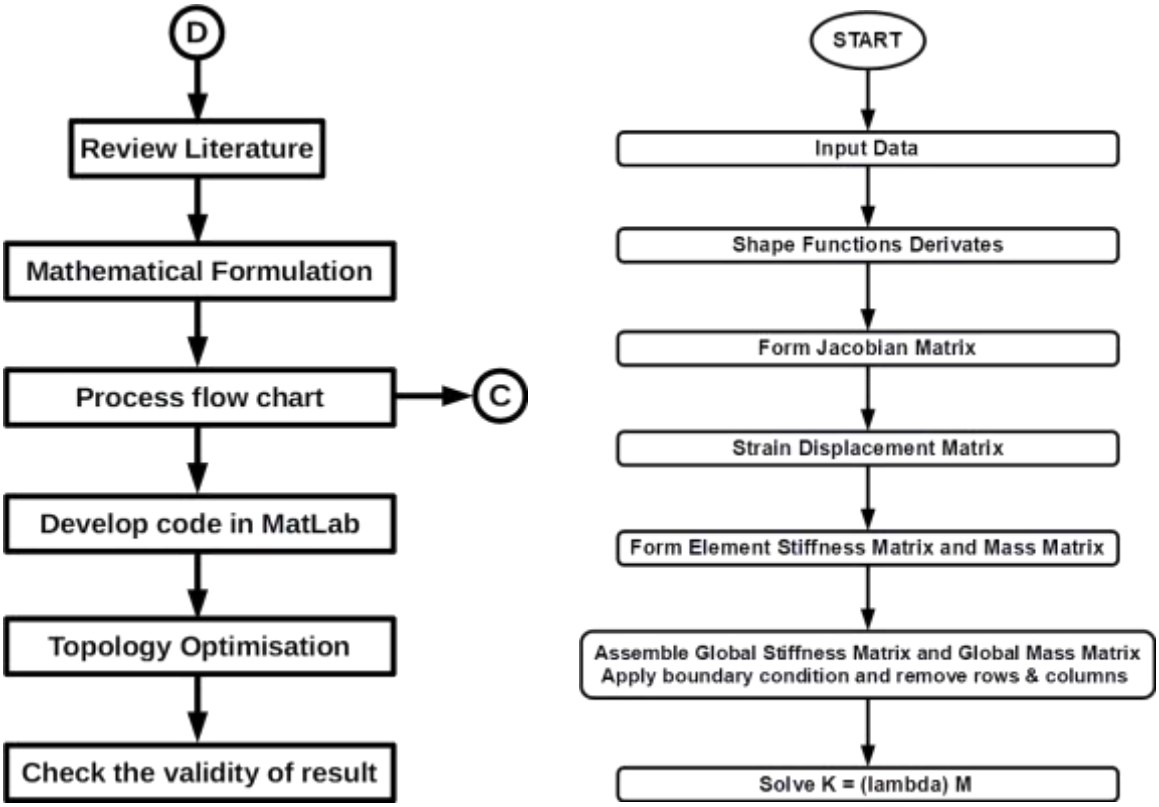


**Fig.5. Flow chart for dynamic analysis.**

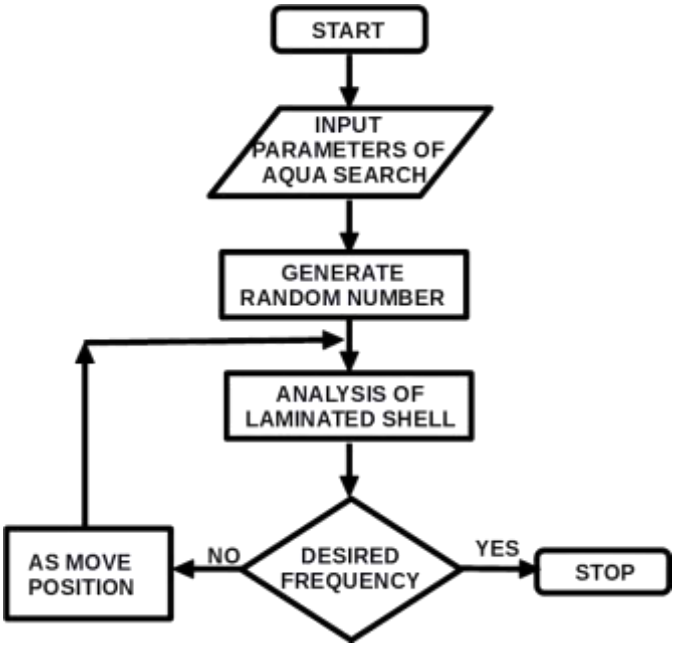


**Fig.6. Optimisation process**

https://doi.org/10.5281/zenodo.18617512

In Fig.6 the random number is generated between from 0 to1. AS indicates aqua search algorithm to generate newer value of the lining factor. The diver moves towards another diver with the better value of objective function. The increase in the value of the lining factor results in the decrease in the natural frequency. In Fig.7 the flow chart shows the regression analysis using five different machine learning algorithms.

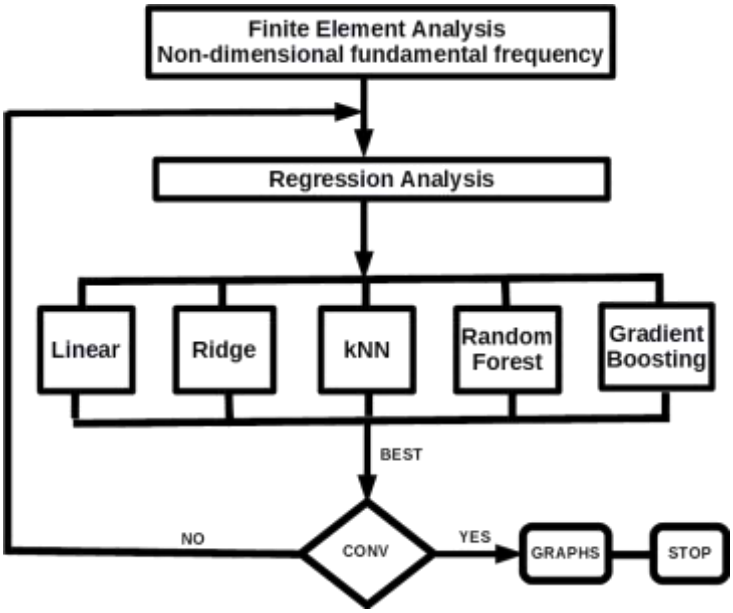


**Fig.7 Flow chart showing Artificial Intelligence and Machine Learning methods**

## 3.1 Theoretical background

### 3.1.1 Aqua search meta-heuristic algorithm

Aqua search is a meta-heuristic algorithm, which is based on underwater sea divers searching in the deep sea. The sea is usually deep and is dark everywhere. The diver will have contact with the base station above using a wire or a wireless GPS device. The diver can use his instinct when choosing the search direction and this instinct helps in making decisions. The visibility of the water in the deep sea is very less and the diver usually has a light over his head which will have certain visibility. The visibility is different for different types of water sometimes clear sometimes not clear. The divers can exchange the information between them with an electronic device. The base station at the surface of the sea keeps track of every movement of the diver. The coordinates of the location and the direction of searching and the step length as well. The base station maintains interactions with everyone.

A weight is assigned to each water body depending on the type of the water body. Some water bodies are easy to search while some of them are not having clear water or have rocky terrain inside the deep sea. The design domain to search is the water body, the divers are the search particles and the search object is the point where all divers ideally should converge.

Sometimes, all the divers may not converge a few of them might converge and others might not. There are cases when the divers are searching in several different directions and cannot reach the convergence point.

The cartesian distance can be calculated similar to the firefly algorithm. There are instructions sent from the base station to the divers. The diver can follow these instructions or use his instinct to make the search direction and take the search step length as well. This factor can is the factor1 which is a base station factor, value close to zero means the diver follows whatever the instructions he receives from the base station. If factor1 is taken as equal to one, then the diver goes by his instinct and his experience and he gives less weightage to the instructions received from the base station. When diver chooses to go by his experience and instinct, then there is another term which accounts for the instinct in the second term. This term is obtained by multiplying the factor1 with a gamma distribution, if needed we can use a random function as well.

The third factor is visibility in the deep sea. The water body is a deep sea, the water may not be clear and the visibility may be poor. The visibility of the human eye is clear up to a distance of 25 cm nearly. The visibility can be accounted by using an F-distribution. The value of degrees of freedom 'm' in the numerator can be taken as equal to 12. The value of the degrees of freedom 'n' in the denominator is taken as equal to 20. The value of sign is taken as positive when a randomly generated number is greater than 0.5. The value of the sign is taken as negative when the a randomly generated number is less than 0.5.

This aqua search meta-heuristic algorithm has very few terms to model the equation of movement of the divers and search for the object in the under water deep sea.

$$term1 = (1 - factor1) * (1 + RR)^{-t}$$

$$where\ (1 - factor1)\ is\ the\ base\ factor\ and\ \text{var}ies\ from\ zero\ to\ one$$

$$\text{Cartesian distance, RR} = \sqrt{\sum_{k=1}^{d} \left(x_{i,k} - x_{j,k}\right)^2} \tag{3}$$

$$term2 = factor1 * rand(0,1)$$

$$term3 = Fd(t) * sign$$

The coordinates of the diver can be identified using an vector x. The size of the vector is the number of unknowns to be determined. The vector set of all $x_i$ at any iteration can be useful to know the distribution of the material inside the design domain which is shown as a water body.

Fd(t) is the F-distribution where 't' is the iteration number. The degrees of freedom in the numerator is m may be taken as equal to 12 and the degrees of freedom in the denominator is 'n' may be taken as equal to 20. Sign is taken as positive unity when a randomly generated is greater than 0.50. Sign is taken as negative unity when a randomly generated is less than 0.50.

The new position $x_j$ for each diver can be determined by using the relation

$$x_j = x_i + (term2 + term1) * (x_j - x_i) + term3 \quad (4)$$

The objection function at each diver is calculated and compared. They have electronic means to exchange the information. The minimum value of the objective function is the diver towards whom all the remaining divers will like to move. The direction and step length can be calculated using the relation given above. Aqua search deep sea search algorithm is very fast converging when compared with other meta-heuristic algorithms such as firefly algorithm.

### 3.1.2 Lining zone

The layers of lamina are arranged in the lining area as shown in the Fig.8 given below.

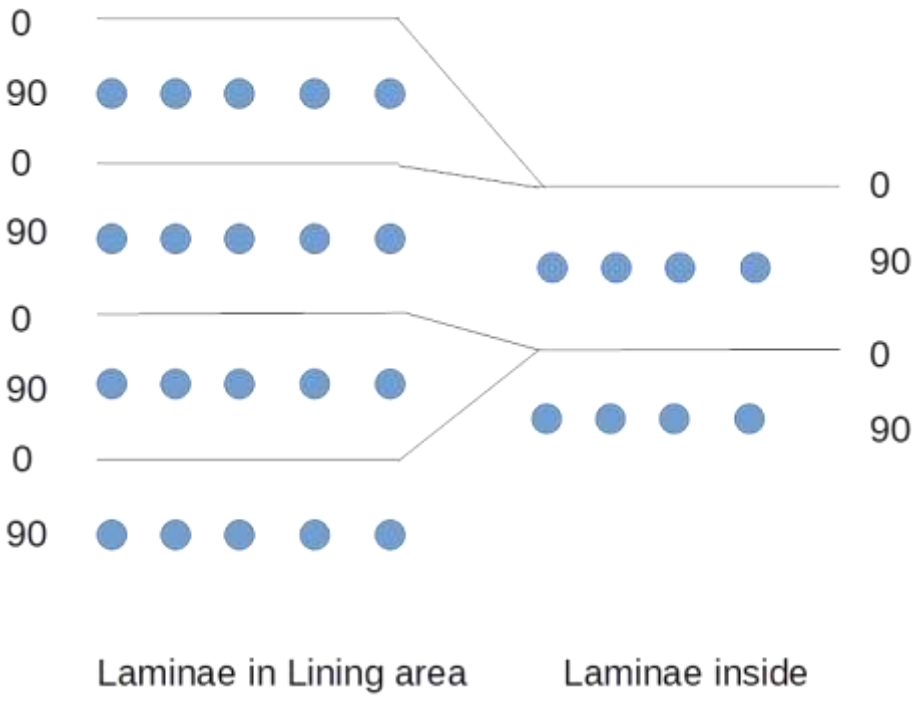


**Fig.8 Arrangement of 0/90/0/90/0/90/0/90 Lamina in the lining area**

The threads in the 90 direction can be closely spaced making the lining area more dense. In the Lining area, the lamina are taken as 0/90/0/90/0/90/0/90 and the modulii of elasticity are multiplied by the lining factor. Lining factor is the ratio of the modulii of elasticity of the material in the lining zone to the modulus of elasticity of the material inside the material domain of the laminate.

https://doi.org/10.5281/zenodo.18617512

In the lining zone, the modulii of elasticity is taken as a multiple of lining factor.

Exx lining zone = 130E3 * Lining factor

Eyy lining zone = 8.5E3 * Lining factor

Gxy lining zone = 6E3 * Lining factor

Gxz lining zone = 6E3 * Lining factor

Gyz lining zone = 3E3 * Lining factor

In other words, the theoretical assumption made here is given below here as follows,

Modulus of elasticity of the element at the openings = Lining factor * Modulus of elasticity of the element

### 3.1.3 Six node triangle diagram

Six node linear strain triangle elements and shape functions for 6N LST [20]

$$N_1 = \zeta(2\zeta - 1)$$
$$N2 = \xi(2\xi - 1)$$
$$N3 = \eta(2\eta - 1)$$
$$N4 = 4\zeta\xi$$
$$N5 = 4\xi\eta$$
$$N6 = 4\zeta\eta$$

### 3.1.4 Formulation of laminated plates

Let $\Omega$ be the domain in $R^2$ by the mid plane of the plate and u, v, w denote the displacement components in x,y,z directions respectively. Using the Kirchoff theory the displacements at any point can be expressed as [19]

$$u(x,y,z) = u_o(x,y) - z\theta_x(x,y)$$

$$v(x,y,z) = v_o(x,y) - z\theta_y(x,y)$$

$$w(x,y,z) = w(x,y) \qquad (5)$$

$$where, \theta_x = \frac{\partial w}{\partial x} \quad and \quad \theta_y = \frac{\partial w}{\partial y}$$

In-plane strains through the following equation

$$\varepsilon = \left[\varepsilon_{xx}, \varepsilon_{yy}, \gamma_{xy}\right]^T = \varepsilon_o + z\kappa$$

where, $\varepsilon_o$, $\kappa$ are the in-plane deformations and curvatures of the middle surface respectively

$$\varepsilon_o = \begin{bmatrix} \frac{\partial}{\partial x} & 0 & 0 \\ 0 & \frac{\partial}{\partial y} & 0 \\ \frac{\partial}{\partial y} & \frac{\partial}{\partial x} & 0 \end{bmatrix} \begin{bmatrix} u_o \\ v_o \\ w \end{bmatrix} \quad and \quad \kappa = \begin{bmatrix} 0 & 0 & -\frac{\partial^2}{\partial x^2} \\ 0 & 0 & -\frac{\partial^2}{\partial y^2} \\ 0 & 0 & -2\frac{\partial^2}{\partial x \partial y} \end{bmatrix} \begin{bmatrix} u_o \\ v_o \\ w \end{bmatrix} \tag{6}$$

Strain displacement matrix is given by

$$b = \begin{bmatrix} \frac{\partial}{\partial x} & 0 & 0 \\ 0 & \frac{\partial}{\partial y} & 0 \\ \frac{\partial}{\partial y} & \frac{\partial}{\partial x} & 0 \\ 0 & 0 & -\frac{\partial^2}{\partial x^2} \\ 0 & 0 & -\frac{\partial^2}{\partial y^2} \\ 0 & 0 & -2\frac{\partial^2}{\partial x \partial y} \end{bmatrix} + \begin{bmatrix} 0 & 0 & \frac{N_i}{R_x} \\ 0 & 0 & \frac{N_i}{R_y} \\ 0 & 0 & 0 \\ 0 & 0 & 0 \\ 0 & 0 & 0 \\ 0 & 0 & 0 \end{bmatrix} = \begin{bmatrix} \frac{\partial}{\partial x} & 0 & -N_i C_{xx} \\ 0 & \frac{\partial}{\partial y} & -N_i C_{yy} \\ \frac{\partial}{\partial y} & \frac{\partial}{\partial x} & 0 \\ 0 & 0 & -\frac{\partial^2}{\partial x^2} \\ 0 & 0 & -\frac{\partial^2}{\partial y^2} \\ 0 & 0 & -2\frac{\partial^2}{\partial x \partial y} \end{bmatrix}$$

https://doi.org/10.5281/zenodo.18617512

In case of a cylindrical shell, the radius of curvature, $R_{xx}$ is infinity and as curvature, $C_{xx}$ is the reciprocal of the radius of curvature, $R_{xx}$ which means that $C_{xx} = 0$. For the sake of our formulation, we consider $C_{yy} = -1/R_{yy}$

$$\overline{Q}_{11} = Q_{11}\cos^4\theta + 2(Q_{12} + 2Q_{66})\sin^2\theta\cos^2\theta + Q_{22}\sin^4\theta$$

$$\overline{Q}_{12} = (Q_{11} + Q_{22} - 4Q_{66})\sin^2\theta\cos^2\theta + Q_{12}(\sin^4\theta + \cos^4\theta)$$

$$\overline{Q}_{16} = (Q_{11} - Q_{12} - 2Q_{66})\sin\theta\cos^3\theta + (Q_{12} - Q_{22} + 2Q_{66})\sin^3\theta\cos\theta$$

$$\overline{Q}_{22} = Q_{11}\sin^4\theta + 2(Q_{12} + 2Q_{66})\sin^2\theta\cos^2\theta + Q_{22}\cos^4\theta$$

$$\overline{Q}_{26} = (Q_{11} - Q_{12} - 2Q_{66})\sin^3\theta\cos\theta + (Q_{12} - Q_{22} + 2Q_{66})\sin\theta\cos^3\theta$$

$$\overline{Q}_{66} = (Q_{11} + Q_{22} - 2Q_{12} - 2Q_{66})\sin^2\theta\cos^2\theta + Q_{66}(\sin^4\theta + \cos^4\theta)$$

with

$$Q_{11} = \frac{E_{11}}{1 - \upsilon_{12}\upsilon_{21}}, \quad Q_{12} = \frac{\upsilon_{12}E_{11}}{1 - \upsilon_{12}\upsilon_{21}}$$

$$Q_{22} = \frac{E_{22}}{1 - \upsilon_{12}\upsilon_{21}}, \quad Q_{44} = G_{13} \qquad (7)$$

$$Q_{55} = G_{23}, \qquad Q_{66} = G_{12}$$

$$\upsilon_{21}E_{11} = \upsilon_{12}E_{22}$$

$E_{11}$ and $E_{22}$ are Young's Modulus of Elasticity parallel and perpendicular to the fibre orientation. $G_{12}$ is the shear modulus and are $\upsilon_{12}$ *and* $\upsilon_{21}$ are Poissons' ratios. As shown in the Fig.9, the layers of lamina are given with the distance is measured from centre of lamina.

https://doi.org/10.5281/zenodo.18617512

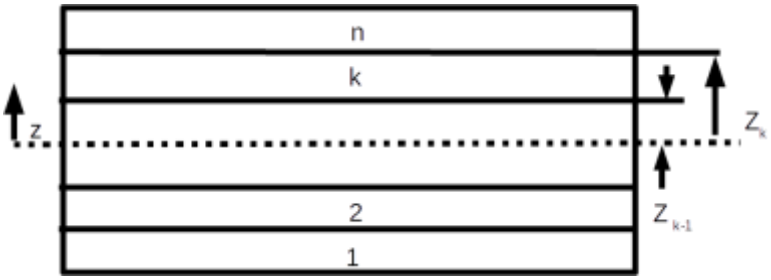


**Fig.9** showing the layers of lamina

$$[E]=\begin{bmatrix} A_{11} & A_{12} & A_{16} & B_{11} & B_{12} & B_{16} \\ A_{21} & A_{22} & A_{26} & B_{21} & B_{22} & B_{26} \\ A_{61} & A_{62} & A_{66} & B_{61} & B_{62} & B_{66} \\ B_{11} & B_{12} & B_{16} & D_{11} & D_{12} & D_{16} \\ B_{21} & B_{22} & B_{26} & D_{21} & D_{22} & D_{26} \\ B_{61} & B_{62} & B_{66} & D_{61} & D_{62} & D_{66} \end{bmatrix}=\begin{bmatrix} A & B \\ B & D \end{bmatrix}$$

$$A_{ij}=\sum_{k=1}^{n}\left(\bar{Q}_{ij}\right)_k\left(z_k-z_{k-1}\right) \qquad B_{ij}=\frac{1}{2}\sum_{k=1}^{n}\left(\bar{Q}_{ij}\right)_k\left(z_k^2-z_{k-1}^2\right)$$

$$D_{ij}=\frac{1}{3}\sum_{k=1}^{n}\left(\bar{Q}_{ij}\right)_k\left(z_k^3-z_{k-1}^3\right) \qquad \text{i, j = 1,2,6} \qquad (8)$$

The value of z is measured from the centre of the lamina as shown in the Fig.14.

The physical and the displacement field are expressed as

$$x^h(\xi,\eta)=\sum_{A}^{nm}R_A(\xi,\eta)P_A$$

$$u^h(x(\xi,\eta))=\sum_{A}^{nm}R_A(\xi,\eta)q_A$$

The strains can be expressed to following nodal displacements as

$$\left[\varepsilon_o \quad \kappa\right]^T=\sum_{A}^{nm}\left[B_A^m \; B_A^b\right]^T q_A$$

$$B_A^m = \begin{bmatrix} R_{A,x} & 0 & 0 \\ 0 & R_{A,y} & 0 \\ R_{A,y} & R_{A,x} & 0 \end{bmatrix} \quad and \quad B_A^b = \begin{bmatrix} 0 & 0 & -R_{A,xx} \\ 0 & 0 & -R_{A,yy} \\ 0 & 0 & -2R_{A,xy} \end{bmatrix}$$

When the radii of curvature are equal to infinity in case of straight edge, and when the curvature is equal to zero

$B_A^m \quad and \quad B_A^b$ are membrane and bending strain displacement matrices using the derivatives of the function

Global stiffness matrix $K = \int_{\Omega} \left\{ \begin{bmatrix} B^m \\ B^b \end{bmatrix}^T \begin{bmatrix} A & B \\ B & D \end{bmatrix} \begin{bmatrix} B^m \\ B^b \end{bmatrix} \right\} d\Omega$

Force vector is $f = \int_{\Omega} pRd\Omega$ (9)

For sinusoidal loading, $p = p_0 \sin(\pi x/a) \sin(\pi y/b)$

**q** is the global displacement vector

### 3.1.4.1 Hygroscopic analysis

The formulation of to determine the force vector is given here below.

Strain Tensor $\begin{bmatrix} \varepsilon_1 \\ \varepsilon_2 \\ \frac{1}{2}\gamma_{12} \end{bmatrix} = [T] \begin{bmatrix} \varepsilon_x \\ \varepsilon_y \\ \frac{1}{2}\gamma_{xy} \end{bmatrix}$ (10)

$$[T] = \begin{bmatrix} \cos^2\theta & \sin^2\theta & 2\sin\theta\cos\theta \\ \sin^2\theta & \cos^2\theta & -2\sin\theta\cos\theta \\ -\sin\theta\cos\theta & \sin\theta\cos\theta & \cos^2\theta - \sin^2\theta \end{bmatrix} \quad (11)$$

https://doi.org/10.5281/zenodo.18617512

$$\begin{bmatrix} \beta_x \\ \beta_y \\ \frac{1}{2}\beta_{xy} \end{bmatrix} = [T^{-1}] \begin{bmatrix} \beta_1 \\ \beta_2 \\ \frac{1}{2}\beta_{12} \end{bmatrix} = \begin{bmatrix} \cos^2\theta & \sin^2\theta & -2\sin\theta\cos\theta \\ \sin^2\theta & \cos^2\theta & 2\sin\theta\cos\theta \\ \sin\theta\cos\theta & -\sin\theta\cos\theta & \cos^2\theta - \sin^2\theta \end{bmatrix} \begin{bmatrix} \beta_1 \\ \beta_2 \\ \frac{1}{2}\beta_{12} \end{bmatrix}$$

where, $\frac{1}{2}\alpha_{12} = \frac{1}{2}\beta_{12} = 0$

Hygro strain = $\begin{bmatrix} \varepsilon_x^{Hy} \\ \varepsilon_y^{Hy} \\ \gamma_{xy}^{Hy} \end{bmatrix} = \begin{bmatrix} \Delta C\beta_x \\ \Delta C\beta_y \\ \Delta C\beta_{xy} \end{bmatrix}$

Total strain = Mechanical strain + Thermal Strain + Hygro strain

$$\begin{bmatrix} \varepsilon_x^{Tot} \\ \varepsilon_y^{Tot} \\ \gamma_{xy}^{Tot} \end{bmatrix} = \begin{bmatrix} \varepsilon_x^{Mech} \\ \varepsilon_y^{Mech} \\ \gamma_{xy}^{Mech} \end{bmatrix} - \begin{bmatrix} \varepsilon_x^{Th} \\ \varepsilon_y^{Th} \\ \gamma_{xy}^{Th} \end{bmatrix} - \begin{bmatrix} \varepsilon_x^{Hy} \\ \varepsilon_y^{Hy} \\ \gamma_{xy}^{Hy} \end{bmatrix} \tag{12}$$

The total strain is given as

$$[\varepsilon^{Tot}] = \begin{bmatrix} \varepsilon_x^{Tot} \\ \varepsilon_y^{Tot} \\ \gamma_{xy}^{Tot} \end{bmatrix} = \begin{bmatrix} \varepsilon_x^0 + zk_x \\ \varepsilon_y^0 + zk_y \\ \gamma_{xy}^0 + zk_{xy} \end{bmatrix} - \begin{bmatrix} \varepsilon_x^{Th} \\ \varepsilon_y^{Th} \\ \gamma_{xy}^{Th} \end{bmatrix} - \begin{bmatrix} \varepsilon_x^{Hy} \\ \varepsilon_y^{Hy} \\ \gamma_{xy}^{Hy} \end{bmatrix} \tag{13}$$

The stress is given as

$$[\sigma] = [\overline{Q}][\varepsilon^{Tot}] = [\overline{Q}](\{\varepsilon^0\} + z\{k\} - \{\varepsilon^{Th}\} - \{\varepsilon^{Hy}\})$$

$$\begin{bmatrix} A & B \\ B & D \end{bmatrix} \begin{bmatrix} \varepsilon^0 \\ k \end{bmatrix} = \begin{bmatrix} N^{Th} \\ M^{Th} \end{bmatrix} + \begin{bmatrix} N^{Hy} \\ M^{Hy} \end{bmatrix} = [F^N]$$

$$(A_{ij}, B_{ij}, D_{ij}) = \int_{-h/2}^{h/2} (1, z, z^2)\overline{Q}_{ij}\, dz \quad i, j = 1, 2, 6 \tag{14}$$

The element level nodal load vector due to hygroscopic forces is given as $\iint [B]^T \{F^N\} dxdy$

## 4.0 Aqua search v/s Firefly algorithm

**Comparison of Aqua Search meta-heuristic algorithm and firefly algorithm meta-heuristic algorithm**

### 4.1 Problem statement to compare fire fly algorithm and aqua search meta-heuristic algorithm:

CCCC laminated composite conoidal shell is having a size of 80 x 80 in plan. The laminate is discretised using six node linear strain triangular elements. The total number of elements are 440 and total number of nodes are 960. A cutout of dimensions 30 x 30 is centrally placed. The elements surrounding the cutout having a width of 2.5. The number of lamina are four with the sequence of 0/90/0/90. The material of the laminate in the lining zone for a width of 2.5 around the cutout is optimised for a desired frequency of the laminate. The lining factor is a multiple of the modulus of elasticity and is determined using Aqua Search meta heuristic algorithm. The objective function is to find the non-dimensional natural frequency of the laminate having the lining along the edge of the cutout. Aqua search (AS) meta-heuristics algorithm is used to determine the optimal lining factors to plot a non-dimensional frequency curve for a given set of geometry ratios. Interpolation curve to determine the non-dimensional frequency using Firefly algorithm is as shown in Fig.10a.

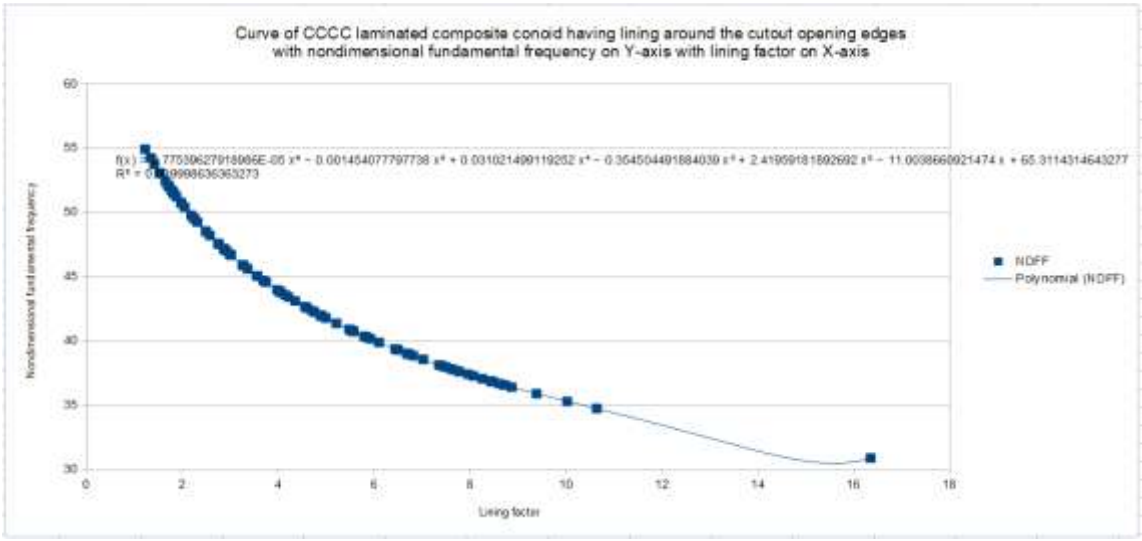


**Fig.10a. Fundamental frequency curve for CCCC laminated composite conoidal shell using firefly algorithm using VC++**

The validation of aqua search meta-heuristic algorithm is done using a conoidal shell. Conoidal shell is considered as the benchmark structure to verify the results obtained from various algorithms used in the analysis of shell structures. Aqua search meta-heuristic algorithm gave better results with least number of search divers in the least possible time.

https://doi.org/10.5281/zenodo.18617512

Firefly algorithm took 5 search flies and 92 iterations and the program continued for nearly 21 hours. Aqua search took 2 search divers and 12 iterations and the program continued for nearly 144 minutes. The convergence criteria is met within a short period of time for aqua search meta-heuristic algorithm.

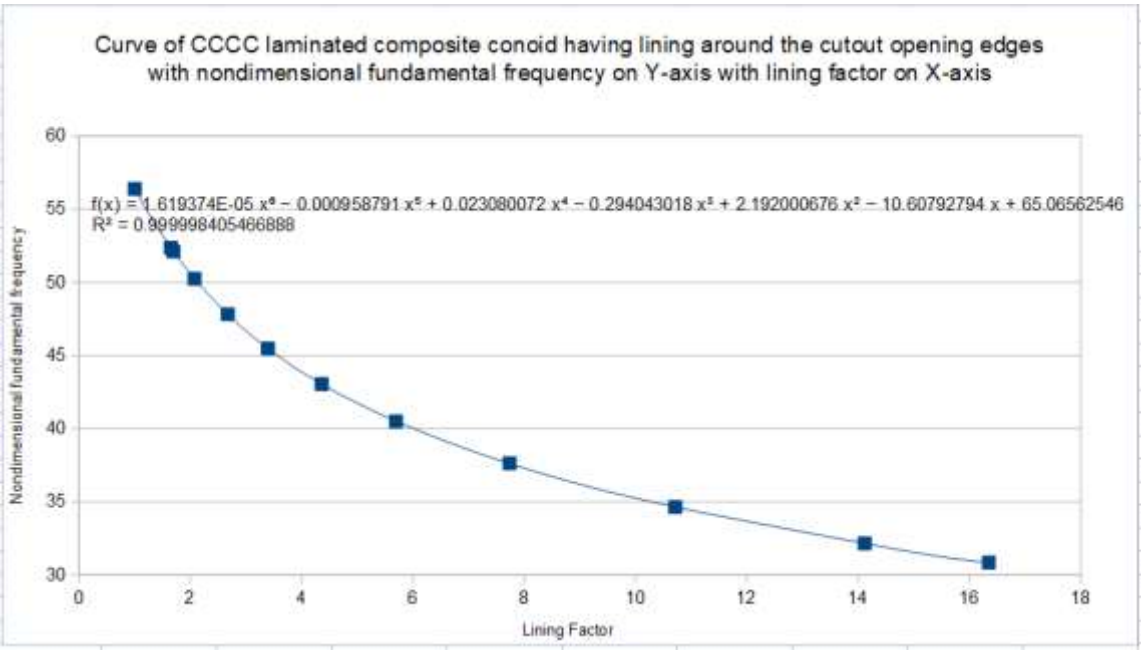


**Fig.10b. Fundamental frequency curve for CCCC laminated composite conoidal shell using aqua search algorithm using VC++**

A characteristic curve showing the natural frequencies of the laminate is developed as shown in Fig.10b. A total of 92 iterations are performed for a duration of 21 hours for firefly algorithm and took 12 iterations for aqua search algorithm to arrive at the curve. The results obtained using AS algorithm are found to be in good agreement with the results obtained using analytical method as shown in Table 1.

**Table 1. Comparison of frequency using aqua search meta-heuristic optimisation, using polynomial relation and using analytical method**

| | Lining Factor | Frequency AS optimisation | Frequency FFA | Frequency Analytical |
|---|---|---|---|---|
| | 5.79111 | 40.3638034 | 40.3486 | 40.3438 |
| Flies/Divers | | 2 | 5 | |
| Iterations | | 12 | 92 | |
| Time | | 144 minutes | 21 hours | |

## 5.0 Analysis

The results of aqua search meta-heuristic algorithm have led us to determine the optimal lining factors. The analysis is done for several cases with different types of loading and boundary conditions. Although the main focus of this paper is frequency analysis, we have checked this lining of laminates approach for every possible case on different types of shells as well.

### Problem statement

A square laminated composite plate is having a dimension of 80 x 80 square which has a cutout of dimension 30 x 30 square at the centre of the plate. The modulus of elasticity of the material is given as $E_{XX}$ = 130E3, $E_{YY}$ = 8.50E3, $G_{XY}$ = 6E3, $G_{XZ}$ = 6E3, $G_{YZ}$ = 3E3, Rho ($\rho$) = 100. The Poisson's ratio is taken as equal to 0.30. There are four layers of lamina which are considered here 0/90/0/90. The elements around the edge of the cutout are having eight layers of lamina 0/90/0/90/0/90/0/90 and the modulii of the elasticity of the material and the density of the material for these elements along the edge of the cutout are multiplied by 20. The plate is meshed using first order six node linear strain triangular elements. The number of elements are 440 and the number of nodes are 968. The number of nodes having support boundary condition are 128. The laminated composite plate is having three different types of supports.

### 5.1 Initial investigation

#### 5.1.1 Uniformly distributed load

##### 5.1.1.1 CCCC laminated plate carrying u.d.l.

Laminated plate carrying a uniformly distributed transverse loading acting vertically downward. The area near to the cutout edges undergoes less deformation as the suitable lining has been provided. The strain energy distribution shows that the support edges are carrying the maximum energy as shown in Fig.11 and the cutout edges are carrying the least. The cutout edges are safe and will not fail or tear apart early.

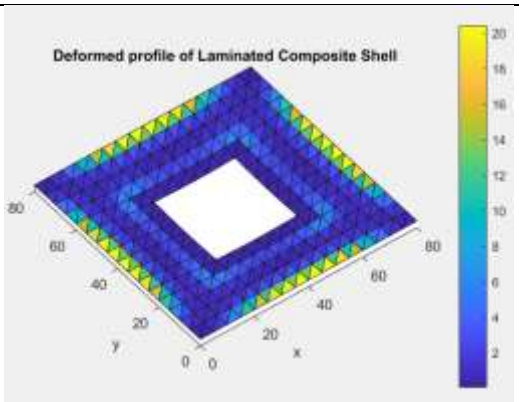


**Fig.11 Distribution of strain energy of a laminated composite plate with lining around the cutout edges and carrying uniformly distributed transverse loading**

### 5.1.1.2 CCCC Laminated composite elliptical shell carrying u.d.l.

Fig.12 shows laminated composite elliptical shell subjected to uniformly distributed transverse loading, the first image on the left is without lining along the cutout edges, the corners are carrying high magnitude of strain energy and hence they are likely to fail first before the laminate starts to take any loading. When the lining is provided along the cutout edges, the edges undergo less deformation and hence they are not carrying higher value of strain energy as shown in the deep blue color. The laminated shell is actually taking the load and undergoes deformation indicated by the strain energy in all the elements. This shows that the laminate is actually taking the load keeping the cutout edges as safe.

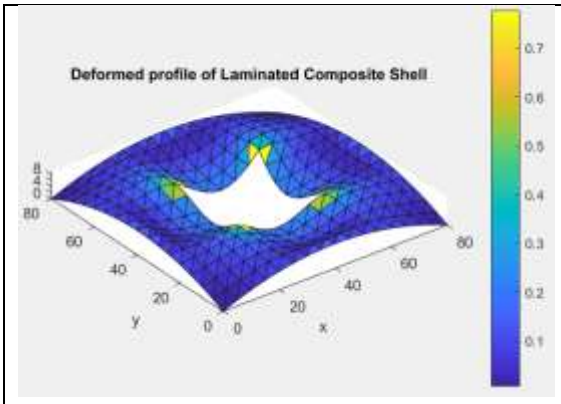


| CCCC elliptical shell carrying transverse loading with out lining | CCCC elliptical shell carrying transverse loading with lining |
|---|---|

**Fig.12 CCCC elliptical shell carrying transverse loading with and without lining**

### 5.1.2 Hygroscopic loading with 1.5% moisture content

Hygroscopic analysis of laminated composites with lining around the cutout opening is performed in this section. Different kinds of shells have been considered in this section namely, plate, conoidal shell, elliptical shell, cylindrical shell and hyperbolic shell with all the four edges as fixed. The loading in this case is 1.5% moisture content.

The deformed profile of a CCCC plate with 1.5% moisture content is as shown in the Fig.13. The strain energy around the cutout edges is the least in deep blue color. The load is actually carried by the laminate and the edges do not fail at the beginning.

| | |
|---|---|
| 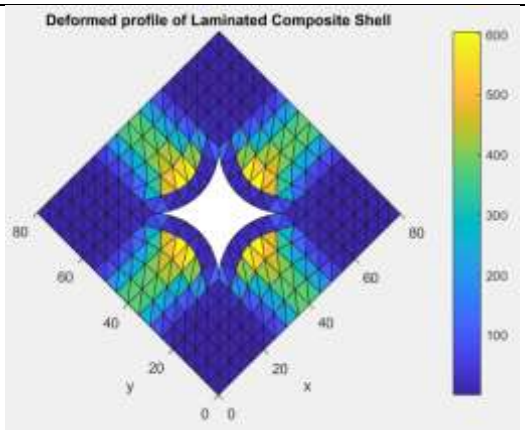  | 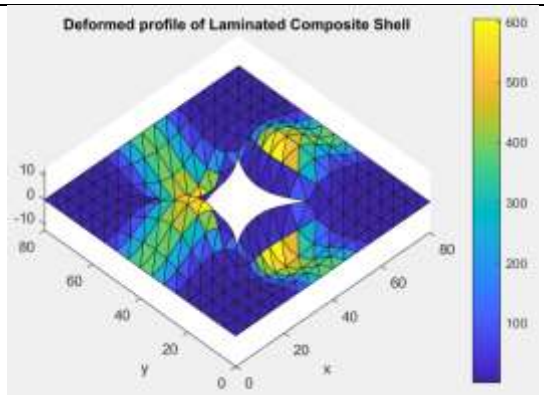  |
| Top view | Isometric side view |

**Fig. 13 Deformed profile of plate with 1.5% moisture content**

| | |
|---|---|
| 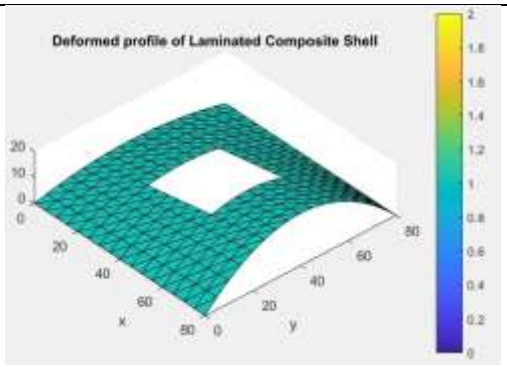  | 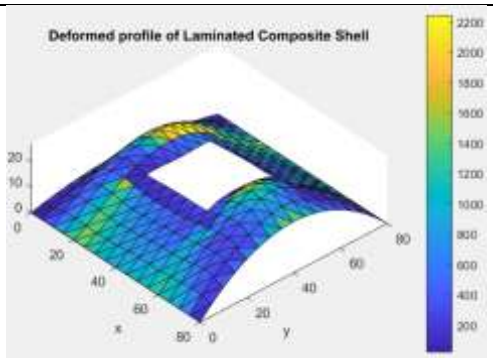  |
| Undeformed profile of conoidal shell | Deformed profile of conoidal shell with 1.5% moisture content |

**Fig.14 Profile of a Conoidal shell carrying 1.5% moisture content**

The undeformed profile of the conoidal shell is shown in the Fig.14 on left side. The shell has a cutout opening and is subjected to 1.5% moisture content as loading. The deformed profile of the conoidal shell is as shown in the Fig.14 on the right side. The cutout edges are in deep blue color shows at the edges the strain energy is less compared to the material inside. This means that the load is carried by the shell and the cutout edges are carrying least strain energy.

Similar is the pattern observed with other kinds of shells namely cylindrical shell, elliptical shell and hyperbolic shell as shown in Fig.15, Fig.16 and Fig.17 given below.

https://doi.org/10.5281/zenodo.18617512

| | |
|---|---|
| 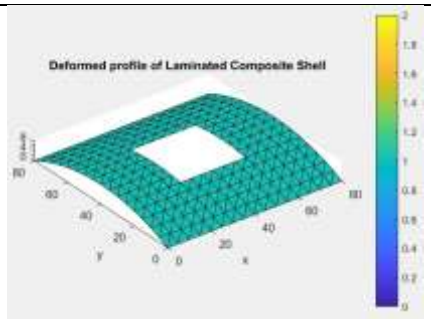  | 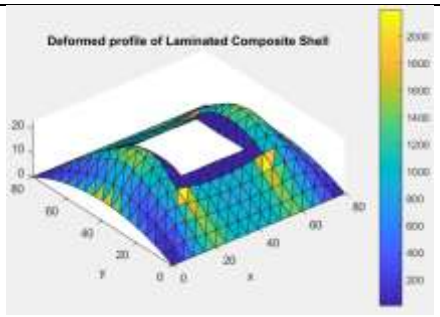  |
| Undeformed profile of cylindrical shell | Deformed profile of cylindrical shell with 1.5% moisture content |

**Fig.15 Deformed profile of a cylindrical shell carrying 1.5% moisture content**

| | |
|---|---|
| 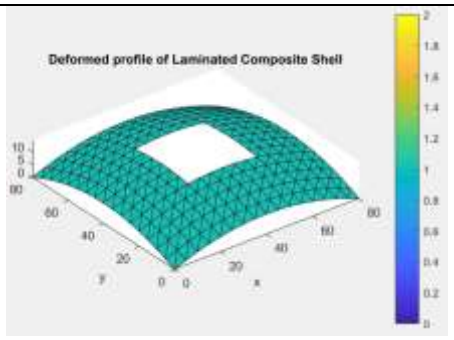  | 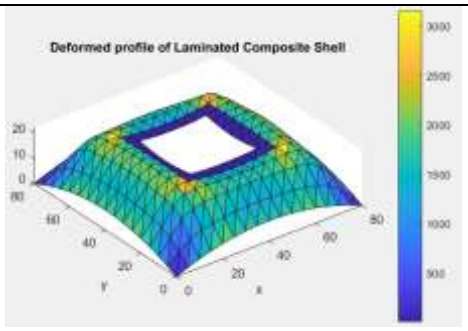  |
| Undeformed profile of elliptical shell | Deformed profile of elliptical shell with 1.5% moisture content |

**Fig.16 Deformed profile of a elliptical shell with (Rx = Ry) carrying 1.5% moisture content**

| | |
|---|---|
| 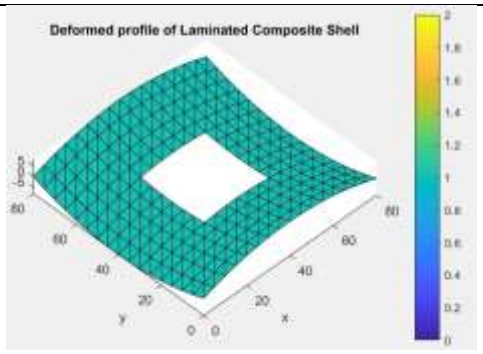  | 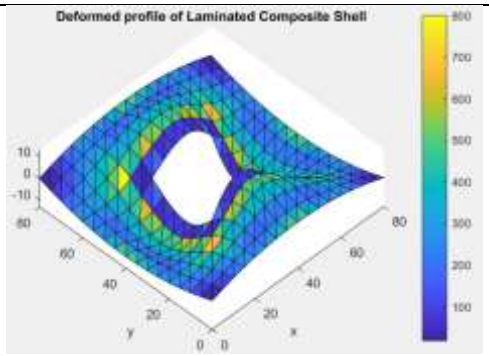  |
| Undeformed profile of hyperbolic shell | Deformed profile of hyperbolic shell with 1.5% moisture content |

**Fig.17 Deformed profile of a hyperbolic shell (Rx = -Ry) carrying 1.5% moisture content**

https://doi.org/10.5281/zenodo.18617512

### 5.1.3 Vibration analysis

First mode of vibration is taken for different kinds of laminated composite shell to measure the non-dimensional fundamental frequency (NDFF). The analysis is done for three different types of support conditions for the laminate, namely all edges of plate are simply supported, clamped, hinged. The results of fundamental frequency, first mode of vibration profile of laminate are shown below for each support condition for both laminated plate with edge stiffening lining and without lining. The results clearly show that the edge stiffening lining measures can reduce the fundamental frequency and also reduce the maximum displacement at node in the first mode of vibration. We consider 0/90/0/90/0/90/0/90 layers for elements along the cutout edge and the value of modulii of elasticity and the density are multiplied by lining factor of 20.

#### 5.1.3.1 SSSS laminated composite plate

The support condition for each node along X-axis is 10110 and the support condition for each node along Y-axis is 01101. The non-dimensional fundamental frequency is 12.3389. The mode shape is as shown in the Fig.18. By increasing the modulii of elasticity and density, the fundamental frequency changes to 8.8082. The maximum displacement in the eigen vector is 6.4392e-04 as shown in the Fig.18.

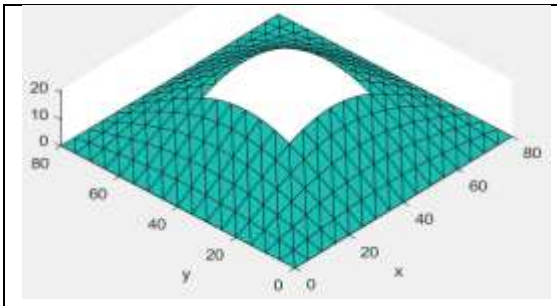


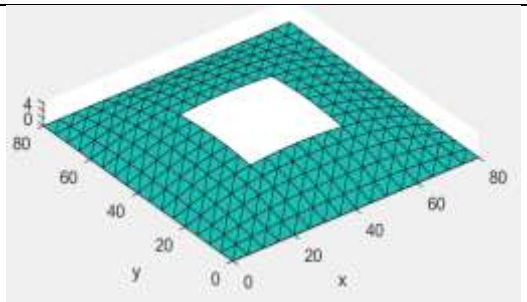


| Without lining of SSSS plate<br>NDFF = 12.3389 | With lining of SSSS plate<br>NDFF = 8.8082 |
|---|---|

**Fig.18 Fundamental mode shape of SSSS laminated plate having cutout**

#### 5.1.3.2 HHHH laminated composite plate

HHHH (Hinged on all four edges)

The support condition for each node along X-axis is 11110 and the support condition for each node along Y-axis is 11101. The non-dimensional fundamental frequency is 12.6368. The maximum absolute value of eigen vector is found to be 0.00214 as shown in the Fig.19. By increasing the modulii of elasticity and density, the fundamental frequency changes to 9.02285. The maximum displacement in the eigen vector is 6.4623e-04 as shown in Fig.19.

https://doi.org/10.5281/zenodo.18617512

| | |
|---|---|
| 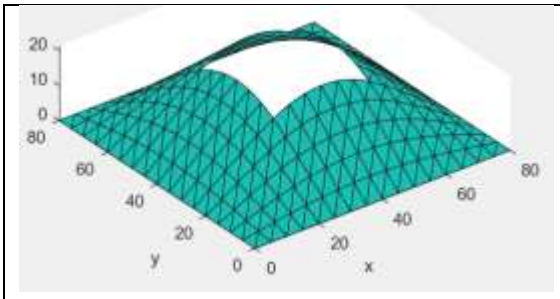 | 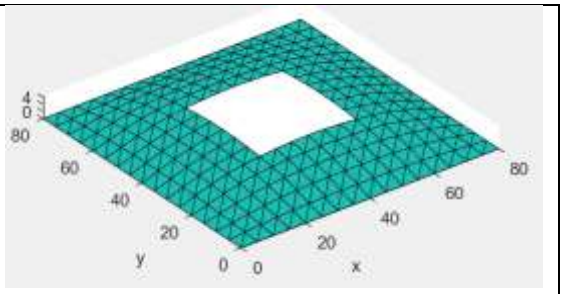 |
| Without lining of HHHH plate<br>NDFF = 12.6368 | With lining of HHHH plate<br>NDFF = 9.02285 |

**Fig.19 Fundamental mode shape of HHHH laminated plate having cutout**

### 5.1.3.3 CCCC laminated composite plate

CCCC (Clamped / fixed on all four edges)

The support condition for each node along X-axis is 11111 and the support condition for each node along Y-axis is 11111. The non-dimensional fundamental frequency is 36.4215. The maximum absolute value of the eigen vector is found to be equal to 0.002753. The fundamental mode shape as shown in the Fig.20 is drawn to a scale of 1 x $10^4$. We can clearly observe the elements along the support boundary nodes are showing no displacement and no rotation as shown in Fig.20. By increasing the modulii of elasticity and density, the fundamental frequency changes to 16.45028. The maximum displacement in the eigen vector is 7.10201e-04. The CCCC support fixity has led to an increase in the fundamental frequency of the laminate higher than the frequency with SSSS and HHHH support condition as shown in Table 2.

| | |
|---|---|
| 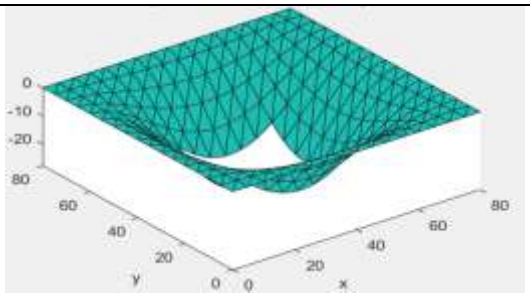 | 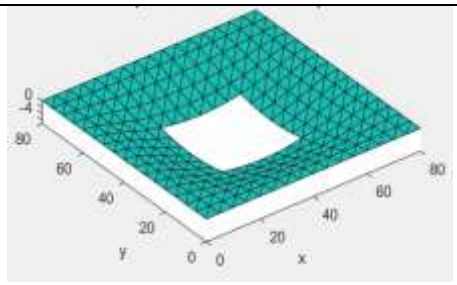 |
| Without lining of CCCC plate<br>NDFF = 36.4215 | With lining of CCCC plate<br>NDFF = 16.45028 |

**Fig.20 Fundamental mode shape of CCCC laminated plate having cutout**

**Table 2 showing the comparison of NDFF of laminated composite plate with different boundary conditions**

| Description | SSSS | HHHH | CCCC |
|---|---|---|---|
| Without Lining | 12.3389 | 12.6368 | 36.4215 |
| With Lining | 8.8082 | 9.02285 | 16.45028 |

### 5.1.4 Vibration analysis of shells

Vibration analysis is performed to determine the non-dimensional fundamental frequency (NDFF) of each kind of shell namely conoidal shell, elliptical shell, hyperbolic shell having fixed boundary conditions.

#### 5.1.4.1 CCCC laminated composite conoidal shell

The first mode of vibration for a CCCC laminated conoidal shell is as shown in Fig.21.

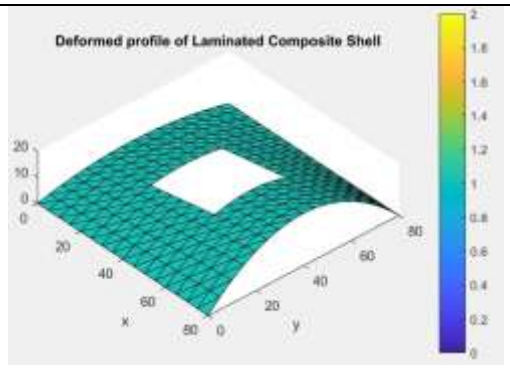


Undeformed profile of conoidal shell

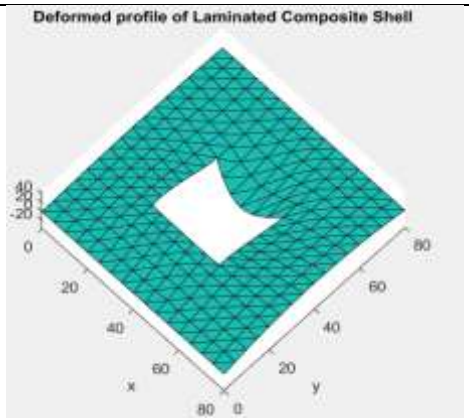


Without lining of conoidal shell
NDFF = 88.277

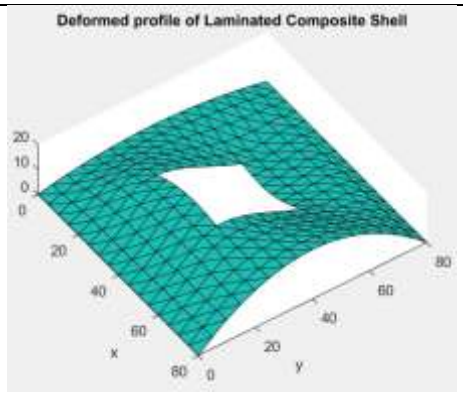


With cutout lining of conoidal shell
NDFF = 45.42

**Fig. 21 Conoidal shell first mode of vibration with and without lining around cutout edges**

The first mode of vibration is as shown in the Fig.21 for the conoidal shell. The image on the left is the first mode of vibration without lining of laminates around the cutout openings. The non-dimensional fundamental frequency is 88.277. When the cutout edges are having the lining of the edges, the first fundamental frequency of vibration is lowered to 45.42. Lining helps to reduce the fundamental frequency and the edges of cutout are strengthened as well.

#### 5.1.4.2 CCCC laminated composite elliptical shell

The first mode of vibration for a CCCC laminated elliptical shell is as shown in Fig.22

<table>
<tr><td colspan="2"> 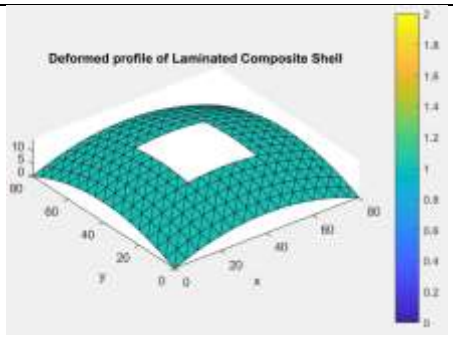
</td></tr>
<tr><td colspan="2">Undeformed profile of elliptical shell</td></tr>
<tr><td> 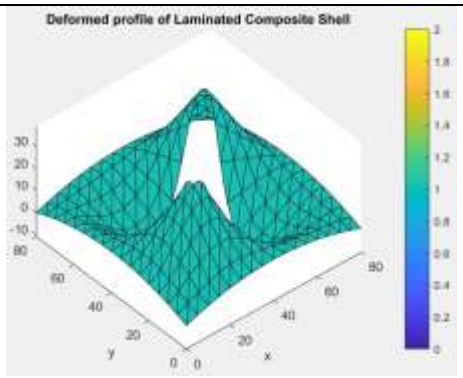
</td><td> 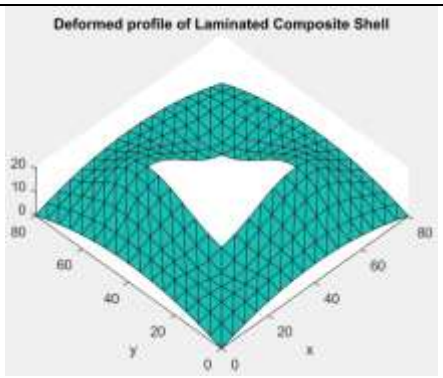
</td></tr>
<tr><td>Without lining of elliptical shell<br>NDFF = 100.742</td><td>With lining of elliptical shell<br>NDFF = 60.458</td></tr>
</table>

**Fig. 22 Elliptical shell first mode of vibration with and without lining around cutout edges**

The elliptical shell with the radius Rx equal to radius Ry is analysed and the fundamental frequency of vibration is determined. The non-dimensional fundamental frequency without lining is found to be 100.742 and with lining it is 60.458. Lining reduces the fundamental frequency of vibration and the edges are kept safe. The amplitude of vibration is lowered with lining the edges of the laminates.

### 5.1.4.3 CCCC laminated composite hyperbolic shell

The first mode of vibration for a CCCC laminated hyperbolic shell is as shown in Fig.23.

<table>
<tr><td colspan="2"> 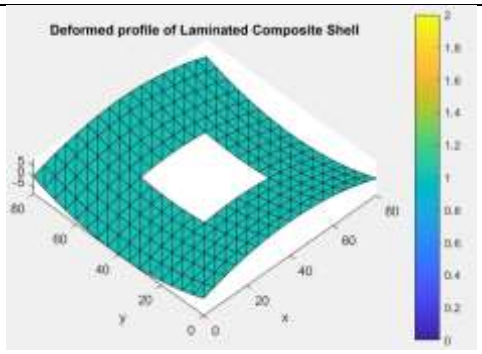
</td></tr>
<tr><td colspan="2">Undeformed profile of hyperbolic shell</td></tr>
<tr><td> 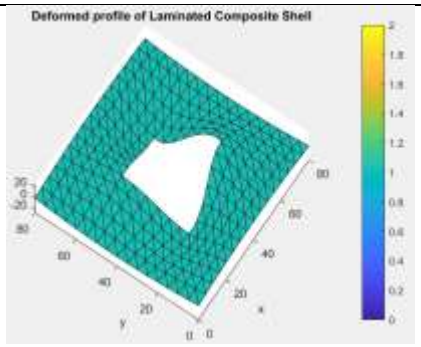
</td><td> 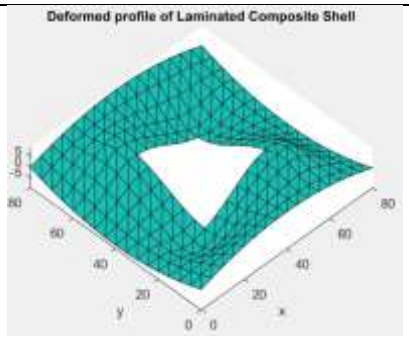
</td></tr>
<tr><td>Without lining of hyperbolic shell<br>NDFF = 117.654</td><td>With lining of hyperbolic shell<br>NDFF = 61.957</td></tr>
</table>

**Fig. 23 Hyperbolic shell first mode of vibration with and without lining around cutout edges**

Similar response of the laminate is observed in case of hyperbolic shells having fixed boundary condition. The non-dimensional frequency without lining the cutout edges is equal to 117.654 and reduces to 61.957 with lining the cutout edges. The amplitude of vibration is lower when the cutout edges are having lining.

This section has done some extensive research on several different types of shell carrying different types of loading and boundary conditions. Every case, the advantages of lining of a laminate cannot be under emphasized. The strength of the laminate has increased, the maximum displacement has reduced in case of transverse loading, lowered the strain energy of elements in the cutout edges, the fundamental frequency of vibration has reduced, the maximum amplitude of vibration has reduced, and the edges are strengthened as well. In the next section, we determine the non-dimensional fundamental frequency of a CCCC laminated composite plate with 0/90/0/90 lamina and 0/90/0/90/0/90/0/90 lamina in the lining area at the cutout edges. NDFF is calculated for several different geometry ratios by varying the length of the edges. The thickness of the laminated plate is kept as equal to one.

### 5.2 Analysis of CCCC laminated composite plate 0/90/0/90 lamina and having 0/90/0/90/0/90/0/90 lamina in the lining along the edge of the opening and by varying geometry ratios

In the previous section, different cases of laminated composite plates and shells for different type of loading and support conditions have been analysed. In this section, we present the non-dimensional fundamental frequency of a 0/90/0/90 CCCC laminated composite plate having lining around the cutout edges with a 0/90/0/90/0/90/0/90 lamina. The transition is smooth between the edge and the inner material of the composite laminate.

#### 5.2.1 Problem statement

A square laminated composite plate is having a dimension of 80 x 80 square which has a cutout of dimension 30 x 30 square at the centre of the plate. The modulus of elasticity of the material is given as $E_{XX}$ = 130E3, $E_{YY}$ = 8.50E3, $G_{XY}$ = 6E3, $G_{XZ}$ = 6E3, $G_{YZ}$ = 3E3, Rho ($\rho$) = 100. The Poisson's ratio is taken as equal to 0.30. There are four layers of lamina which are considered here 0/90/0/90. The elements around the edge of the cutout are having eight layers of lamina 0/90/0/90/0/90/0/90 and the modulii of the elasticity of the material and the density of the material for these elements along the edge of the cutout are multiplied by lining factor. The plate is meshed using first order six node linear strain triangular elements. The number of elements are 440 and the number of nodes are 968. The number of nodes having support boundary condition are 128. The laminated composite plate is having fixed or clamped support on all sides.

Several geometry ratios which are considered here are the ratio of the edge1 to edge2 which are 0.25, 0.50, 0.75, 1.0, 1.25, 1.50, 1.75, 2.0. There are different values of the edge1 which are considered 50, 80, 100, 120, 160, 200. The thickness of the laminate is uniform throughout the laminate and is equal to unity. The optimal lining factors given by aqua search meta-heuristic algorithm are 16.3462, 1.69558, 1, 1.64888, 2.07497, 2.67246, 3.39439, 4.35938, 5.69433, 7.73602, 10.714, 14.1174. The ratio of the edge1 to the thickness of the laminate is taken as numerically equal to the value of the edge1 in plan of the laminated composite shell. The values of lining factor obtained from aqua search meta-heuristic algorithm have been used and the non-dimensional fundamental frequency are determined. The shell is discretised using six node linear strain traingular elements. Finite element analysis is done to determine the stiffness matrix (K) and mass matrix (M) and then the fundamental frequencies are determined as eigen values of the stiffness matrix and mass matrix. The eigen values are then transformed into non-dimensional fundamental frequencies. The first eigen frequency is usually the highest value and the first mode of vibration can be determined. The first mode shape for several different shells have been presented in the earlier section. A scatter plot of these NDFF for the case of composite laminated plate for different values of the lining factors have been presented. The scatter plot is drawn in google colabs. The coding is done using python and machine learning classes are imported and the scatter plot is drawn as shown in Fig.24.

https://doi.org/10.5281/zenodo.18617512

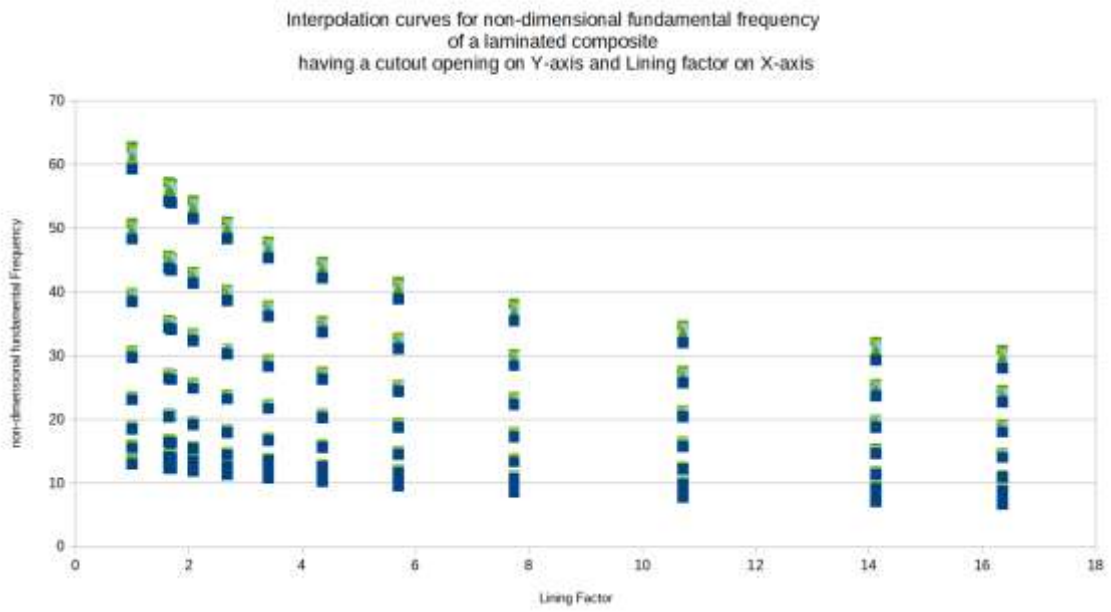


**Fig.24. Scatter plot of non-dimensional fundamental frequency characteristic for CCCC 0/90/0/90 laminated composite plate having cutout and 0/90/0/90/0/90/0/90 lining along the cutout edges using 6N LST FEM code for different aspect ratios (a/b = 0.25, 0.50, 0.75, 1.0, 1.25, 1.50, 1.75, 2.0)**

In the next section, we have applied five machine learning methods namely linear regression, ridge regression, k nearest neighbour, random forest, and gradient boosting methods.

### 5.3 Apply AIML techniques

In the previous section, a scatter plot is used to show the variation of non-dimensional fundamental frequency for different geometry ratios and lining factors. In this section, machine learning methods are applied to determine the NDFF and evaluate the performance metrics and choose the best method.

Five different methods have been applied using artificial intelligence and machine learning (AIML) methods namely

- Linear Regression (LR)
- Ridge Regression (RR)
- kNearest Neighbour (kNN)
- Random Forest (RF)
- Gradient Boosting (GB)

Five machine learning methods namely linear regression, ridge regression, k nearest neighbour, random forest, and gradient boosting methods to interpolate and determine the value of non-dimensional fundamental frequencies for several geometry aspect ratios of

edge1 to edge2 equal to 0.25, 0.50, 0.75, 1.0, 1.25, 1.50, 1.75, 2.0 and the value of edge1 are taken as equal to 60,70,90,100,110,130,140,150,170,180,190. The ratio of edge1 to thickness of laminate is taken as equal to unity for all geometry ratios. The coding has been done in python in Google Colabs® and the results are compared. The performance metrics chosen are mean absolute error, root mean square error and the $R^2$ values. Table 3 given below shows the comparison of these performance metrics. Clearly the best method is gradient boosting which is giving least error and higher $R^2$ value.

**Table 3 Comparison of performance metrics of different AIML algorithms**

| Method | MAE | RMSE | $R^2$ Score |
|---|---|---|---|
| Linear Regression (LR) | 6.8898 | 8.4996 | 0.5887 |
| Ridge Regression (RR) | 6.8898 | 8.4996 | 0.5887 |
| kNearest Neighbour (kNN) | 1.0637 | 1.946 | 0.9784 |
| Random Forest (RF) | 0.2545 | 0.431 | 0.9989 |
| Gradient Boosting (GB) | 0.168 | 0.2336 | 0.9997 |

MAE - Mean Absolute Error

RMSE - Root Mean Square Error

The graph shows the mean absolute error (MAE) for each method and compares with the error in x-axis and model in y-axis. Linear regression and ridge regression are having highest error and gradient boosting is the best method with the least value of MAE. Gradient boosting is better than other methods with least mean absolute error as shown in Fig.25.

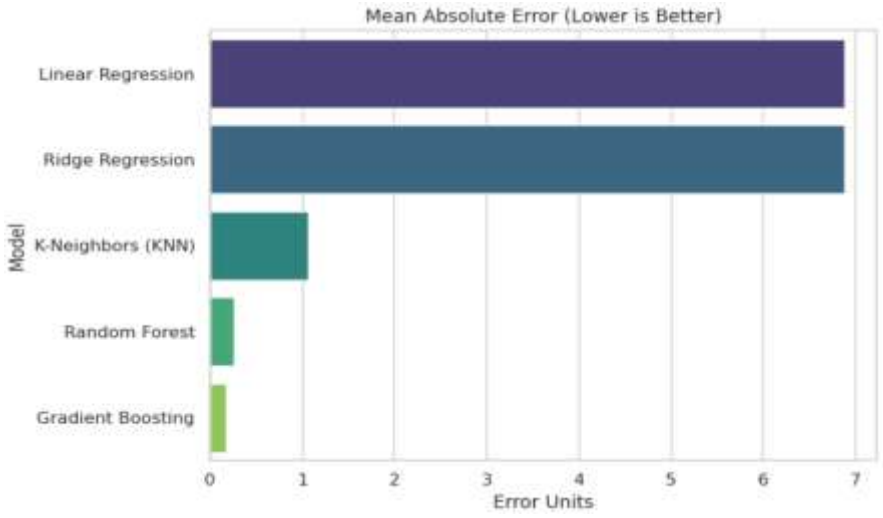


**Fig. 25 Mean absolute error for five different machine learning methods**

The R2 accuracy score graph clearly shows that gradient boosting is having a highest value of 99.9% and Linear regression has the least accuracy. Gradient boosting is the best method among all five methods as shown in the Fig.26.

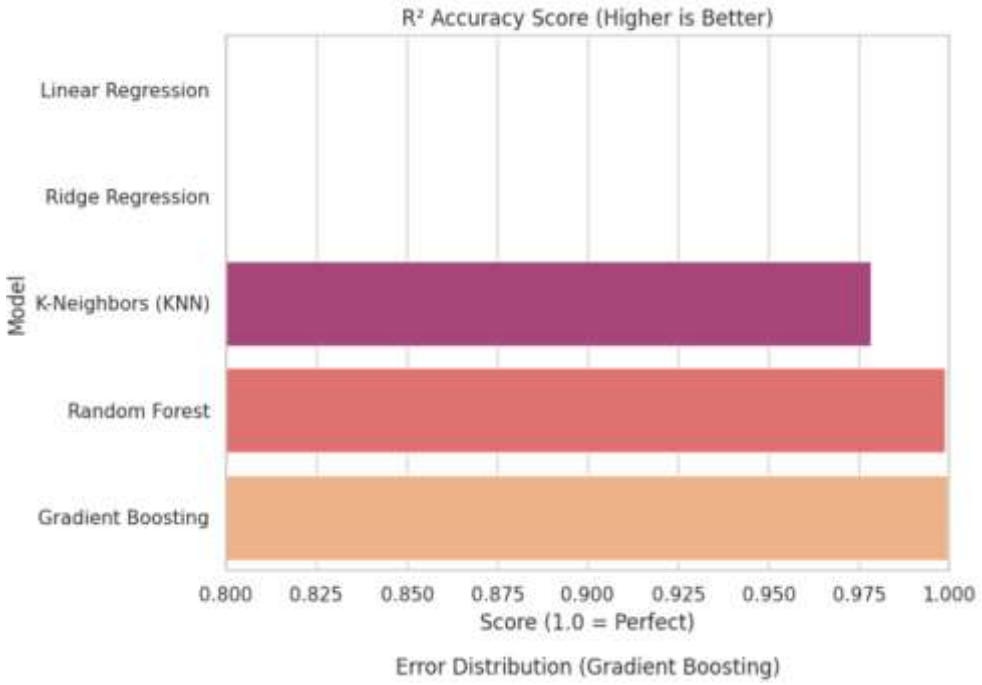


**Fig. 26 accuracy score for five different machine learning methods**

The graph in Fig.27 shows the comparative measure of predicted value with actual value. The scatter in green color is aligns along the best fit curve with Gradient boosting. The scatter in red color is linear regression which is the worst fit method.

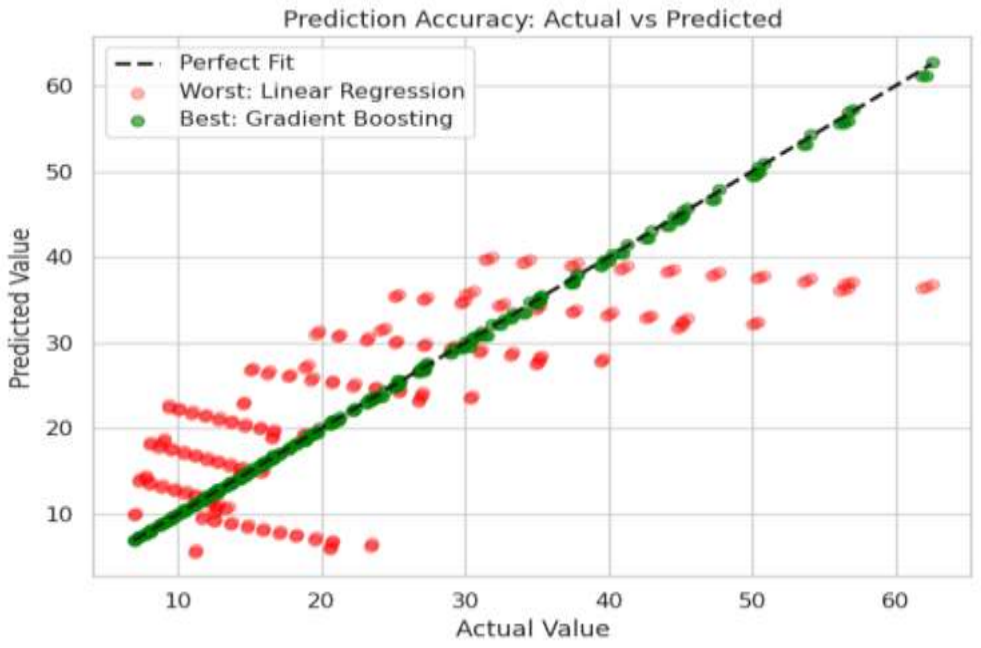


**Fig.27 Comparison of accuracy for best method and worst method**

The error distribution in gradient boosting is normal distribution curve and as shown in the Fig.28 . The error distribution is shown in columns with maximum count at the centre and least at the extremes.

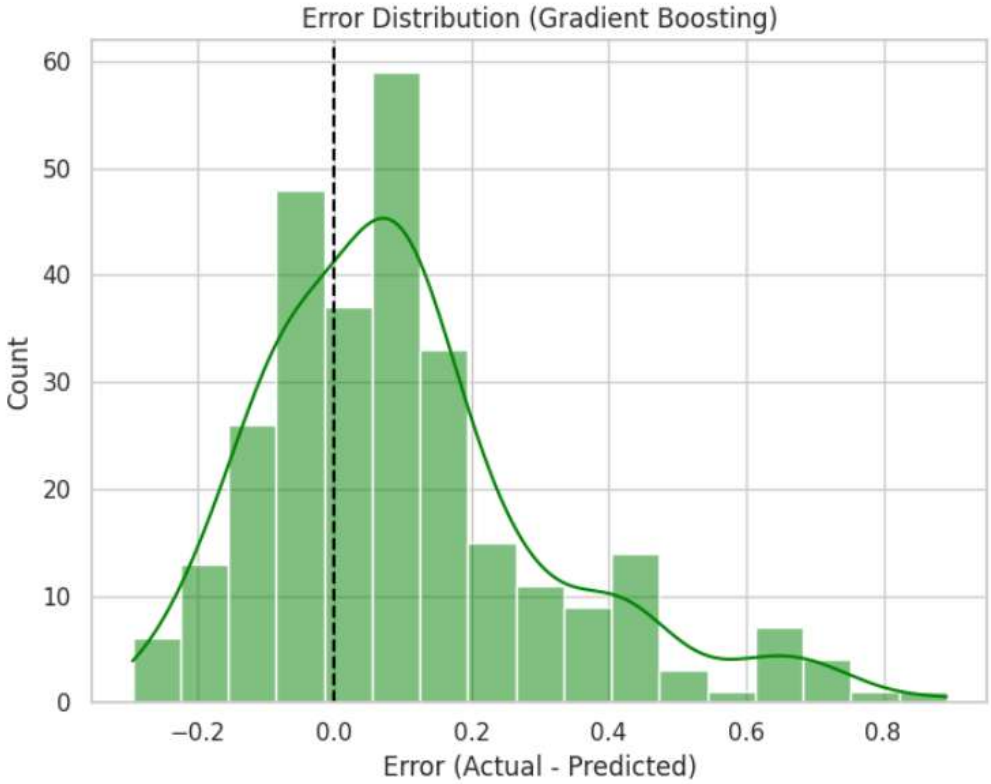


**Fig.28 Error distribution using gradient boosting**

A random check has been done to verify the validity of the methods. A combination of geometry ratios is chosen at random whose non-dimensional fundamental frequency is determined by using finite element analysis. For a/b = 1.5, and a/h = 200 and lining factor = 2.67246.

The graph is drawn for the given set of ratio for different lining factors and the polynomial equal is fit to these data points as shown in Fig.29. This polynomial equation is having a highest degree of seven. This polynomial equation is specific for this geometry ratio chosen and is also used to find the value of non-dimensional fundamental frequency for the given set of geometry ratios and lining factor.

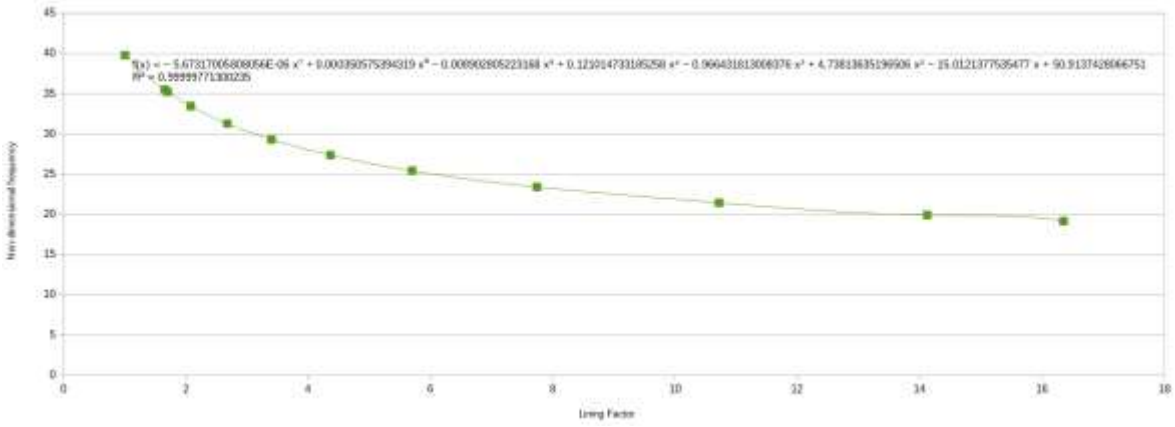

**Fig.29 CCCC laminated composite plate having lining at the cutout edges and analysed using FEM analysis for the ratios of edge a = 200, a/b =1.5, a/h = 1**

For the same set of geometry ratios the non-dimensional fundamental frequency is determined by applying AIML Gradient boosting method and determine the non-dimensional fundamental frequency for 0/90/0/90 CCCC laminated composite plate having cutout and lining along the opening as shown in Table 4 given below.

**Table 4 Comparison of NDFF using FEM, Gradient boosting, polynomial equation**

| a = 200<br>b = 133.33 | a/b | Lining Factor | Using polynomial equation | Using AIML GB techniques | Using FEM |
|---|---|---|---|---|---|
| | 1.5 | 2.67246 | 31.269649 | 31.25283 | 31.2864 |
| % Error | | | -0.05354 % | -0.10729 % | |

https://doi.org/10.5281/zenodo.18617512

## 6.0 Summary and Conclusions

This research study in this paper is focused on lining of the laminated plate along the edge of the cutout. Several different type of loading conditions are checked and for different kinds of shells. In case of plates, three different support conditions were considered, namely SSSS, HHHH, CCCC. The fundamental frequency of vibration and the maximum displacement at node in the first mode of vibration were measured in each case. We observed with increase in the fixity the fundamental frequency of vibration has increased and the clamped plate has the maximum value of fundamental frequency. This is due to the increase in the stiffness of element having higher number of layers. As the stiffness increases the fundamental frequency increases and as the stiffness reduces the fundamental frequency reduces. Similarly, as the stiffness increase the displacement reduces, and as the stiffness reduces the displacement increases. As the mass increases the fundamental frequency reduces. With lining of laminates along the edges of the cutout, the frequency has reduced and the displacement at node in the fundamental frequency of vibration has been reduced as well. This proves that the edges along the cutout can be strengthened by lining and the longevity of the laminate might increase as well.

The results obtained from optimisation are in good agreement with the analytical results. The natural frequency of a laminated composite shell with lining around the cutout edges has been optimised for optimal lining factor. A check has been made for a geometry ratio of 1.5 and lining factor of 2.67246, the non-dimensional fundamental frequency using finite element analysis is found to be 31.2864. The results of finite element analysis using six node linear strain triangle are in close agreement with those obtained using artificial intelligence and machine learning algorithms which is 31.25283. The data points obtained from the aqua search meta-heuristic algorithm are curve fitted using a seventh degree polynomial curve. The polynomial curve is used to determine the non-dimensional fundamental frequency and is in close agreement with the values obtained from finite element analysis. Five different machine learning models are used namely, Linear Regression (LR), Ridge Regression(RR), kNearest Neighbours (kNN), Random Forest (RF), Gradient Boosting (GB). Out of these five methods, Gradient Boosting (GB) is the best method and the Linear Regression (LR) model is the worst model. Three measures have been used to evaluate the performance of these models namely Mean Absolute Error (MAE), Root Mean Square Error (RMSE), $R^2$ value. The least error for Gradient Boosting (GB) is found to be nearly 0.1%. The complete data of non-dimensional fundamental frequency for different lining factors and geometry aspect ratio is given in Appendix A using both finite element analysis and machine learning gradient boosting methods.

### 6.1 Future study

i. Non-linear reliability based topology optimisation of laminated composite shell structures having cutout opening and with the cutout edges are having lining and subjected to dynamic loading.

https://doi.org/10.5281/zenodo.18617512

## References


1. Sarmila Sahoo Performance evaluation of free vibration of laminated composite stiffened hyperbolic paraboloid shell panel with cutout, International Journal of Emerging Technologies, 2016, Vol.7, pp.1-24, ISSN: 2297-623X, SciPressLtd., Switzerland. https://doi.org/10.18052/www.scipress.com/IJET.7.1
2. Maharudra, Bheemsha Arya, T.Rajanna Buckling behaviour of composite laminates of trapezoidal panel with cutout subjected to non-uniform in-plane edge loads, Materials Today: 2020, Proceedings, https://doi.org/10.1016/j.matpr.2020.09.224
3. Sundarajan Natarajan, Pratik S. Deogekar Hygrothermal effects on free vibration and buckling of laminated composites with cutouts, Composite Structures, 2013, Vol.108, pp.848-855. https://doi.org/10.1016/j.compstruct.2013.10.00 9
4. Aydin Komur et. al. Buckling analysis of laminated composite plates with an elliptical/circular cutout using FEM. Advances in Engineering Software, 2009, **41,** 161–164
5. Hachemi & S. M. Hamza-Cherif Free vibration of composite laminated plate with complicated cutout, Mechanics Based Design of Structures and Machines, **48(2)**, 192-216, Taylor & Francis 2020. DOI: 10.1080/15397734.2019.1633341
6. Harsh kumar bharadwaj Study of free vibration analysis of laminated composite plates having triangular cutouts Engineering Solid Mechanics, 2015, **3**, 43-50
7. Mohammed Salih Free Vibration Analysis of Perforated Laminated Composite Square Plates Journal of University of Babylon for Engineering Sciences, 2018, **26 (10)**
8. Ahmad Akbari Rahimabadi et.al. Vibration of functionally graded material plates with cutouts & cracks in thermal environment, Key Engineering Materials, **560**, 157-180, 2013. https://doi.org/10.4028/www.scientific.net/KEM.560.157
9. Sreelatha V. Experimental study on shear strengthening of RC T-beams with web openings using FRP Composites, January 2013, National Institute of Technology Rourkela
10. Yu Gao Enhancement of composite open-hole tensile strength via fine Z-pins arrangements, International Journal of Mechanical Sciences 236, 2022, 107752. https://doi.org/10.1016/j.ijmecsci.2022.107752
11. Oskana and Andrey Using Machine learning to predict the stress-strain state of a rectangular plate with a cutout, 2020 CEUR-ws.org/ Vol-2791/2020200001.pdf
12. Lakshmi narayana et.al. Thermal buckling analysis of laminated composite plate with square/rectangular, elliptical/circular cutout, 7th International conference on materials processing and characterisation, Materials Today: Proceedings 5(2018) 5354-5363.
13. El Kiri Y, Zahiri L, Mansouri K, Mighouar Z. Assessment of the harmfulness of corrosion defects in a pressurized pipeline with a single corrosion defect using FEA and ANN. Res. Eng. Struct. Mater., 2025; 11(5): 2307-2330.
14. Serenaj A, Elezi E, Serenaj A. Structural optimization of reinforced concrete spatial structures with different structural openings and forms. Res. Eng. Struct. Mat., 2018; 4(2): 79-89.
15. Ramesh V, Pandulu G, Khanam N, Lian O C. Compressive strength prediction of ecofriendly recycled aggregate concrete: A machine learning approach. Res. Eng. Struct. Mater., 2025; 11(6): 2965-2982.
16. Abdellatif B, Chikh B, Ahmed M. Seismic response prediction using a hybrid unsupervised and supervised machine learning in case of 3D RC frame buildings. Res. Eng. Struct. Mater., 2024; 10(4): 1373-1397.

17. Arun B R, Srishaila J M, Md Khalid S, Algur V, Kavyashree K,Tanu H M. Prediction of machine learning application in the development of novel sustainable self-compacting geopolymer concrete. Res. Eng. Struct. Mater., 2025; 11(4): 1469-1490.

18. Tarun Kant, Swaminathan Analytical solutions for the static analysis of laminated composite and sandwich plates based on a higher order refined theory, Computers Structures, 2002: 56:329-344

19. KNV Chandrasekhar et.al. Cubic b-splines for isogeometric analysis of laminated composite plates subjected to hygroscopic loading using classical laminated plate theory, Journal of Polymer & Composites, 2021, Vol.9, Issue 3, pp.19-32. doi: 10.37591/JoPC

20. KNV Chandrasekhar and Sriram S “Free vibration analysis of laminated composite conoidal shells using six node linear strain triangle elements," i-managers journal on structural engineering, Vol. 8, no. 3, September - November 2019, ISSN 2278-7887

## Appendix A

Non-dimensional fundamental frequency of CCCC laminated composite plate with lining around the cutout edges using FEM and ML Gradient Boosting

| | | Finite Element Analysis | | | | | | Machine Learning Gradient Boosting method | | | | | |
|---|---|---|---|---|---|---|---|---|---|---|---|---|---|
| LiningFactor | a/b | 50 | 80 | 100 | 120 | 160 | 200 | 50 | 80 | 100 | 120 | 160 | 200 |
| 16.3462 | 1 | 10.912121 | 11.121100 | 11.184978 | 11.229165 | 11.292560 | 11.341080 | 10.909112 | 11.130308 | 11.191704 | 11.246608 | 11.316168 | 11.356404 |
| 1.69558 | 1 | 20.261930 | 20.476300 | 20.544518 | 20.598165 | 20.679160 | 20.748710 | 20.250700 | 20.473178 | 20.551598 | 20.594196 | 20.689997 | 20.762196 |
| 1 | 1 | 23.079157 | 23.309800 | 23.391745 | 23.451300 | 23.543840 | 23.621900 | 23.070929 | 23.285345 | 23.371796 | 23.425117 | 23.487170 | 23.608243 |
| 1.64888 | 1 | 20.386918 | 20.622600 | 20.693073 | 20.746665 | 20.829560 | 20.900232 | 20.395552 | 20.603711 | 20.695217 | 20.741823 | 20.806368 | 20.872466 |
| 2.07497 | 1 | 19.199414 | 19.409800 | 19.478186 | 19.527683 | 19.603000 | 19.667913 | 19.201531 | 19.409690 | 19.472660 | 19.519267 | 19.600563 | 19.658695 |
| 2.67246 | 1 | 17.915602 | 18.118400 | 18.180254 | 18.229365 | 18.301480 | 18.363508 | 17.908916 | 18.116263 | 18.179234 | 18.225841 | 18.303841 | 18.361973 |
| 3.39439 | 1 | 16.755026 | 16.961100 | 17.024588 | 17.070368 | 17.141480 | 17.199158 | 16.751262 | 16.958040 | 17.021010 | 17.067617 | 17.142285 | 17.200416 |
| 4.35938 | 1 | 15.634153 | 15.831600 | 15.894643 | 15.938955 | 16.007280 | 16.062008 | 15.650630 | 15.844637 | 15.905070 | 15.944989 | 16.019656 | 16.077787 |
| 5.69433 | 1 | 14.521670 | 14.719400 | 14.781871 | 14.826060 | 14.891760 | 14.944788 | 14.509105 | 14.703112 | 14.763545 | 14.803464 | 14.878131 | 14.936263 |
| 7.73602 | 1 | 13.358127 | 13.558700 | 13.621223 | 13.664520 | 13.728880 | 13.779543 | 13.366070 | 13.555632 | 13.613548 | 13.653466 | 13.728133 | 13.786265 |
| 10.714 | 1 | 12.235209 | 12.440000 | 12.502550 | 12.546315 | 12.609720 | 12.659133 | 12.240943 | 12.440859 | 12.498775 | 12.538693 | 12.613360 | 12.672014 |
| 14.1174 | 1 | 11.357016 | 11.565000 | 11.628643 | 11.672475 | 11.735840 | 11.784677 | 11.346697 | 11.576267 | 11.634183 | 11.674101 | 11.748768 | 11.802489 |
| 16.3462 | 0.25 | 6.712518 | 6.858400 | 6.912600 | 6.954700 | 7.021500 | 7.075720 | 6.712996 | 6.942567 | 6.964753 | 6.930747 | 7.108139 | 7.117017 |
| 1.69558 | 0.25 | 12.284572 | 12.464900 | 12.546200 | 12.620200 | 12.760100 | 12.894091 | 12.335384 | 12.518025 | 12.543506 | 12.605359 | 12.707108 | 12.876385 |
| 1 | 0.25 | 12.954217 | 13.158200 | 13.259992 | 13.358800 | 13.550900 | 13.737483 | 12.958228 | 13.108621 | 13.237932 | 13.337498 | 13.497274 | 13.676714 |

https://doi.org/10.5281/zenodo.18617512

| | | | | | | | | | | | | | |
|---|---|---|---|---|---|---|---|---|---|---|---|---|---|
| 1.64888 | 0.25 | 12.328711 | 12.510800 | 12.593164 | 12.668300 | 12.810400 | 12.946806 | 12.383316 | 12.517950 | 12.589200 | 12.648992 | 12.752579 | 12.909102 |
| 2.07497 | 0.25 | 11.928243 | 12.102000 | 12.177846 | 12.245600 | 12.370900 | 12.488943 | 11.965427 | 12.100062 | 12.171312 | 12.231103 | 12.328921 | 12.478385 |
| 2.67246 | 0.25 | 11.409518 | 11.581600 | 11.653347 | 11.715100 | 11.823500 | 11.920541 | 11.426460 | 11.561094 | 11.629049 | 11.679425 | 11.811891 | 11.961356 |
| 3.39439 | 0.25 | 10.866776 | 11.034100 | 11.099460 | 11.153200 | 11.242600 | 11.317579 | 10.908594 | 11.091064 | 11.122485 | 11.142494 | 11.192818 | 11.283654 |
| 4.35938 | 0.25 | 10.244420 | 10.400200 | 10.457521 | 10.502900 | 10.575400 | 10.634635 | 10.283476 | 10.465947 | 10.495570 | 10.508327 | 10.512281 | 10.572743 |
| 5.69433 | 0.25 | 9.524099 | 9.669300 | 9.721601 | 9.761700 | 9.825100 | 9.876548 | 9.515505 | 9.636463 | 9.718068 | 9.818430 | 9.860300 | 9.852026 |
| 7.73602 | 0.25 | 8.666289 | 8.806200 | 8.856687 | 8.895600 | 8.957100 | 9.007217 | 8.639211 | 8.760170 | 8.836911 | 8.927336 | 9.036111 | 9.000770 |
| 10.714 | 0.25 | 7.772985 | 7.914000 | 7.965750 | 8.006000 | 8.069700 | 8.121936 | 7.717552 | 7.856202 | 7.957288 | 8.025647 | 8.173162 | 8.135034 |
| 14.1174 | 0.25 | 7.065139 | 7.209100 | 7.262580 | 7.304100 | 7.370100 | 7.423957 | 7.034683 | 7.221669 | 7.296383 | 7.355758 | 7.527032 | 7.471051 |
| 16.3462 | 0.5 | 7.502935 | 7.655000 | 7.706584 | 7.744700 | 7.802500 | 7.847884 | 7.435302 | 7.603057 | 7.677772 | 7.744845 | 7.916119 | 7.860138 |
| 1.69558 | 0.5 | 14.047180 | 14.194100 | 14.247322 | 14.290800 | 14.363400 | 14.428789 | 14.067287 | 14.227445 | 14.278925 | 14.294954 | 14.286245 | 14.398415 |
| 1 | 0.5 | 15.540024 | 15.714900 | 15.789271 | 15.848100 | 15.952500 | 16.047360 | 15.545391 | 15.685704 | 15.749157 | 15.800945 | 15.841766 | 16.003453 |
| 1.64888 | 0.5 | 14.132700 | 14.281200 | 14.336993 | 14.379900 | 14.454000 | 14.520584 | 14.205930 | 14.369892 | 14.365159 | 14.386742 | 14.327980 | 14.481633 |
| 2.07497 | 0.5 | 13.410092 | 13.545000 | 13.593205 | 13.631400 | 13.696500 | 13.754240 | 13.412748 | 13.506649 | 13.571897 | 13.613503 | 13.653880 | 13.770866 |
| 2.67246 | 0.5 | 12.582818 | 12.709500 | 12.755201 | 12.790600 | 12.848800 | 12.900441 | 12.542118 | 12.644132 | 12.709380 | 12.782710 | 12.887946 | 12.937450 |
| 3.39439 | 0.5 | 11.799176 | 11.926100 | 11.970250 | 12.003600 | 12.058500 | 12.105502 | 11.749587 | 11.914172 | 11.976425 | 12.000954 | 12.104612 | 12.118341 |
| 4.35938 | 0.5 | 11.006298 | 11.131700 | 11.174417 | 11.207000 | 11.259900 | 11.304636 | 10.970718 | 11.123286 | 11.180622 | 11.205151 | 11.294111 | 11.312031 |
| 5.69433 | 0.5 | 10.195248 | 10.324000 | 10.368548 | 10.401500 | 10.454100 | 10.497842 | 10.167454 | 10.316674 | 10.374010 | 10.398538 | 10.481706 | 10.502623 |
| 7.73602 | 0.5 | 9.329519 | 9.464400 | 9.510656 | 9.544800 | 9.598400 | 9.642039 | 9.311226 | 9.459345 | 9.516681 | 9.541209 | 9.621442 | 9.644587 |

| | | | | | | | | | | | | | |
|---|---|---|---|---|---|---|---|---|---|---|---|---|---|
| 10.714 | 0.5 | 8.486762 | 8.629400 | 8.677953 | 8.713900 | 8.769200 | 8.813642 | 8.484311 | 8.638190 | 8.695526 | 8.720054 | 8.800435 | 8.823579 |
| 14.1174 | 0.5 | 7.831164 | 7.980500 | 8.031160 | 8.068600 | 8.125600 | 8.170687 | 7.868547 | 8.028061 | 8.088203 | 8.112731 | 8.195829 | 8.204852 |
| 16.3462 | 0.75 | 8.756900 | 8.915300 | 8.966000 | 9.002300 | 9.056400 | 9.098900 | 8.757862 | 8.891979 | 8.960819 | 8.997600 | 9.099959 | 9.137073 |
| 1.69558 | 0.75 | 16.305900 | 16.460500 | 16.515200 | 16.557100 | 16.625100 | 16.684700 | 16.346658 | 16.480775 | 16.515255 | 16.539519 | 16.590623 | 16.679535 |
| 1 | 0.75 | 18.507000 | 18.669100 | 18.731900 | 18.782100 | 18.862400 | 18.933100 | 18.496998 | 18.664018 | 18.687040 | 18.697324 | 18.769717 | 18.858630 |
| 1.64888 | 0.75 | 16.419200 | 16.575900 | 16.634100 | 16.675500 | 16.743900 | 16.804600 | 16.441756 | 16.608776 | 16.631797 | 16.635106 | 16.707499 | 16.780616 |
| 2.07497 | 0.75 | 15.466900 | 15.614500 | 15.666100 | 15.707000 | 15.770400 | 15.826500 | 15.475809 | 15.642829 | 15.665850 | 15.669159 | 15.741552 | 15.808316 |
| 2.67246 | 0.75 | 14.437000 | 14.583100 | 14.631700 | 14.671100 | 14.730800 | 14.783700 | 14.442159 | 14.609179 | 14.632200 | 14.635509 | 14.707902 | 14.774666 |
| 3.39439 | 0.75 | 13.513300 | 13.654700 | 13.702800 | 13.739600 | 13.797200 | 13.846600 | 13.509324 | 13.676344 | 13.710253 | 13.725815 | 13.798209 | 13.862506 |
| 4.35938 | 0.75 | 12.604200 | 12.741800 | 12.789100 | 12.824400 | 12.880600 | 12.927500 | 12.630881 | 12.740966 | 12.774875 | 12.814174 | 12.886567 | 12.950864 |
| 5.69433 | 0.75 | 11.694700 | 11.839000 | 11.886800 | 11.921500 | 11.976100 | 12.021100 | 11.718333 | 11.828418 | 11.862327 | 11.912458 | 11.984851 | 12.049148 |
| 7.73602 | 0.75 | 10.747700 | 10.894100 | 10.941700 | 10.977100 | 11.030900 | 11.074500 | 10.772963 | 10.883049 | 10.948517 | 10.998648 | 11.014085 | 11.078382 |
| 10.714 | 0.75 | 9.831700 | 9.983100 | 10.032300 | 10.068400 | 10.122000 | 10.164800 | 9.845989 | 9.950876 | 10.026173 | 10.107253 | 10.122689 | 10.186986 |
| 14.1174 | 0.75 | 9.117300 | 9.273900 | 9.324200 | 9.360400 | 9.414300 | 9.456900 | 9.143395 | 9.252039 | 9.360255 | 9.452164 | 9.462593 | 9.529254 |
| 16.3462 | 1.25 | 14.032800 | 14.386900 | 14.488500 | 14.556100 | 14.646900 | 14.713000 | 14.045387 | 14.383657 | 14.481878 | 14.548441 | 14.642829 | 14.715853 |
| 1.69558 | 1.25 | 26.239900 | 26.601900 | 26.710400 | 26.786500 | 26.891600 | 26.977200 | 26.243081 | 26.607145 | 26.712352 | 26.778915 | 26.873303 | 26.957220 |
| 1 | 1.25 | 29.743900 | 30.219900 | 30.334200 | 30.413100 | 30.542800 | 30.644400 | 29.738883 | 30.187555 | 30.292953 | 30.335867 | 30.500085 | 30.571024 |
| 1.64888 | 1.25 | 26.383600 | 26.801100 | 26.904600 | 26.976000 | 27.085400 | 27.172400 | 26.391692 | 26.799983 | 26.904116 | 26.924660 | 27.080284 | 27.152652 |
| 2.07497 | 1.25 | 24.871700 | 25.233600 | 25.336100 | 25.400800 | 25.502600 | 25.585200 | 24.858864 | 25.236241 | 25.340374 | 25.421167 | 25.497248 | 25.573000 |

| | | | | | | | | | | | | | |
|---|---|---|---|---|---|---|---|---|---|---|---|---|---|
| 2.67246 | 1.25 | 23.212100 | 23.558900 | 23.657000 | 23.722900 | 23.818000 | 23.895500 | 23.239443 | 23.558618 | 23.655393 | 23.727509 | 23.803590 | 23.879342 |
| 3.39439 | 1.25 | 21.719000 | 22.053300 | 22.148000 | 22.213700 | 22.307600 | 22.379800 | 21.744845 | 22.064021 | 22.149430 | 22.211577 | 22.287658 | 22.363410 |
| 4.35938 | 1.25 | 20.251700 | 20.575400 | 20.672000 | 20.735300 | 20.825700 | 20.896000 | 20.248467 | 20.562698 | 20.681214 | 20.743362 | 20.819442 | 20.895194 |
| 5.69433 | 1.25 | 18.781700 | 19.117200 | 19.212000 | 19.276100 | 19.365200 | 19.433200 | 18.776595 | 19.089273 | 19.214969 | 19.315327 | 19.372179 | 19.447931 |
| 7.73602 | 1.25 | 17.254600 | 17.590200 | 17.686200 | 17.749900 | 17.839700 | 17.906000 | 17.251194 | 17.563872 | 17.689568 | 17.789926 | 17.846777 | 17.922529 |
| 10.714 | 1.25 | 15.774800 | 16.117700 | 16.216200 | 16.281600 | 16.371500 | 16.437400 | 15.771509 | 16.093623 | 16.219320 | 16.319678 | 16.376529 | 16.459305 |
| 14.1174 | 1.25 | 14.620700 | 14.968800 | 15.069400 | 15.136000 | 15.226600 | 15.292700 | 14.666775 | 14.982022 | 15.105166 | 15.192057 | 15.248908 | 15.340047 |
| 16.3462 | 1.5 | 18.015600 | 18.626400 | 18.800800 | 18.911600 | 19.053600 | 19.150500 | 18.027488 | 18.594053 | 18.808138 | 18.892405 | 19.005572 | 19.096711 |
| 1.69558 | 1.5 | 34.076900 | 34.696700 | 34.873300 | 34.988400 | 35.131000 | 35.244900 | 34.154399 | 34.688158 | 34.926693 | 35.010960 | 35.146184 | 35.237323 |
| 1 | 1.5 | 38.455000 | 39.128500 | 39.360000 | 39.477400 | 39.654300 | 39.791200 | 38.400436 | 39.151915 | 39.304188 | 39.462792 | 39.598017 | 39.701211 |
| 1.64888 | 1.5 | 34.321700 | 34.922600 | 35.121900 | 35.229400 | 35.375800 | 35.491000 | 34.355463 | 34.949426 | 35.099722 | 35.256570 | 35.391794 | 35.467390 |
| 2.07497 | 1.5 | 32.374900 | 32.954800 | 33.121400 | 33.228300 | 33.362300 | 33.467400 | 32.308069 | 32.910178 | 33.133395 | 33.290243 | 33.425467 | 33.497188 |
| 2.67246 | 1.5 | 30.241400 | 30.795800 | 30.950100 | 31.054500 | 31.186700 | 31.286400 | 30.107633 | 30.709742 | 30.932959 | 31.089806 | 31.225030 | 31.296752 |
| 3.39439 | 1.5 | 28.281300 | 28.825600 | 28.989100 | 29.085300 | 29.215300 | 29.308900 | 28.219035 | 28.760170 | 28.988660 | 29.145507 | 29.280731 | 29.352452 |
| 4.35938 | 1.5 | 26.345900 | 26.885100 | 27.043800 | 27.135000 | 27.264700 | 27.356900 | 26.295614 | 26.812272 | 27.040762 | 27.197609 | 27.332833 | 27.404555 |
| 5.69433 | 1.5 | 24.390700 | 24.945100 | 25.104700 | 25.199900 | 25.329300 | 25.421300 | 24.407366 | 24.946018 | 25.115585 | 25.185689 | 25.320913 | 25.405461 |
| 7.73602 | 1.5 | 22.343300 | 22.904600 | 23.065700 | 23.167800 | 23.298700 | 23.391200 | 22.378789 | 23.068156 | 23.068529 | 23.068170 | 23.203394 | 23.290152 |
| 10.714 | 1.5 | 20.353300 | 20.933900 | 21.101300 | 21.206700 | 21.342500 | 21.436800 | 20.385911 | 21.070825 | 21.121049 | 21.205374 | 21.260730 | 21.380660 |
| 14.1174 | 1.5 | 18.797500 | 19.400400 | 19.571500 | 19.681400 | 19.821000 | 19.917100 | 18.888182 | 19.574692 | 19.628360 | 19.723207 | 19.770058 | 19.978902 |

| | | | | | | | | | | | | | |
|---|---|---|---|---|---|---|---|---|---|---|---|---|---|
| 16.3462 | 1.75 | 22.707400 | 23.717900 | 24.005800 | 24.185500 | 24.406500 | 24.549400 | 22.580337 | 23.795090 | 24.021391 | 24.204267 | 24.392975 | 24.448019 |
| 1.69558 | 1.75 | 43.392200 | 44.425300 | 44.742400 | 44.917900 | 45.138600 | 45.290900 | 43.417302 | 44.305519 | 44.747270 | 44.975905 | 45.245847 | 45.300891 |
| 1 | 1.75 | 48.314800 | 49.574600 | 49.939000 | 50.167100 | 50.446400 | 50.658400 | 48.301726 | 49.246636 | 49.887285 | 50.139941 | 50.565894 | 50.641142 |
| 1.64888 | 1.75 | 43.696400 | 44.763400 | 45.034400 | 45.214200 | 45.436100 | 45.592900 | 43.726552 | 44.534059 | 45.027108 | 45.242535 | 45.571351 | 45.651637 |
| 2.07497 | 1.75 | 41.332300 | 42.324200 | 42.589500 | 42.759500 | 42.961900 | 43.106900 | 41.403363 | 42.282748 | 42.531934 | 42.704237 | 42.983753 | 43.113857 |
| 2.67246 | 1.75 | 38.659600 | 39.625100 | 39.876400 | 40.044100 | 40.232600 | 40.367500 | 38.698809 | 39.667090 | 39.876875 | 40.049178 | 40.188331 | 40.320533 |
| 3.39439 | 1.75 | 36.197300 | 37.116000 | 37.371600 | 37.529800 | 37.715400 | 37.845300 | 36.209666 | 37.159862 | 37.369646 | 37.541949 | 37.685097 | 37.817299 |
| 4.35938 | 1.75 | 33.701300 | 34.603900 | 34.857900 | 35.007600 | 35.194300 | 35.321100 | 33.719634 | 34.608271 | 34.855351 | 35.034494 | 35.179702 | 35.314166 |
| 5.69433 | 1.75 | 31.150400 | 32.070400 | 32.318600 | 32.476100 | 32.668400 | 32.796100 | 31.117017 | 32.083387 | 32.330467 | 32.509610 | 32.659523 | 32.800587 |
| 7.73602 | 1.75 | 28.437000 | 29.378800 | 29.638100 | 29.800500 | 29.999100 | 30.130300 | 28.491035 | 29.371740 | 29.607940 | 29.807377 | 29.982966 | 30.139740 |
| 10.714 | 1.75 | 25.792500 | 26.765700 | 27.041300 | 27.211000 | 27.418700 | 27.555700 | 25.727101 | 26.798019 | 27.082436 | 27.209260 | 27.439798 | 27.570111 |
| 14.1174 | 1.75 | 23.739700 | 24.736900 | 25.021400 | 25.197900 | 25.414400 | 25.556100 | 23.643346 | 24.988060 | 25.177900 | 25.195409 | 25.347603 | 25.529039 |
| 16.3462 | 2 | 28.007900 | 29.561500 | 30.012500 | 30.287400 | 30.620400 | 30.826600 | 28.072499 | 29.516219 | 29.879694 | 30.222144 | 30.651519 | 30.856946 |
| 1.69558 | 2 | 53.972600 | 55.631000 | 56.057200 | 56.325000 | 56.655000 | 56.874900 | 54.009375 | 55.638513 | 56.001988 | 56.344438 | 56.731783 | 56.934852 |
| 1 | 2 | 59.315100 | 61.202200 | 61.776900 | 62.080100 | 62.504500 | 62.812600 | 59.333370 | 61.086092 | 61.787817 | 62.093320 | 62.348232 | 62.829711 |
| 1.64888 | 2 | 54.210900 | 55.943700 | 56.393300 | 56.659600 | 56.995900 | 57.225400 | 54.257597 | 55.880453 | 56.304003 | 56.659459 | 57.061496 | 57.246020 |
| 2.07497 | 2 | 51.524200 | 53.124900 | 53.558900 | 53.801200 | 54.105400 | 54.301700 | 51.528063 | 53.129873 | 53.499013 | 53.800000 | 54.142375 | 54.301296 |
| 2.67246 | 2 | 48.424600 | 49.883200 | 50.287800 | 50.518000 | 50.798700 | 50.982900 | 48.405053 | 49.905812 | 50.279109 | 50.545590 | 50.798290 | 50.957211 |
| 3.39439 | 2 | 45.342300 | 46.787900 | 47.174400 | 47.405500 | 47.683600 | 47.860500 | 45.343889 | 46.850015 | 47.182972 | 47.404920 | 47.658357 | 47.821384 |

| | | | | | | | | | | | | | |
|---|---|---|---|---|---|---|---|---|---|---|---|---|---|
| 4.35938 | 2 | 42.199300 | 43.619600 | 44.014300 | 44.241100 | 44.516400 | 44.687200 | 42.214142 | 43.676103 | 43.988140 | 44.237367 | 44.506535 | 44.682955 |
| 5.69433 | 2 | 38.953800 | 40.375500 | 40.776600 | 41.011800 | 41.291600 | 41.469600 | 38.911369 | 40.391613 | 40.811001 | 41.017107 | 41.299699 | 41.456335 |
| 7.73602 | 2 | 35.442500 | 36.911200 | 37.317300 | 37.562900 | 37.856300 | 38.041200 | 35.437382 | 36.916165 | 37.337277 | 37.558290 | 37.860526 | 38.044920 |
| 10.714 | 2 | 32.020000 | 33.520500 | 33.947600 | 34.206200 | 34.517800 | 34.711800 | 32.026236 | 33.515335 | 33.951915 | 34.217869 | 34.524685 | 34.715725 |
| 14.1174 | 2 | 29.347600 | 30.881200 | 31.325500 | 31.597000 | 31.922600 | 32.124900 | 29.357104 | 30.888333 | 31.346615 | 31.610814 | 31.933201 | 32.132924 |